MAGNETIC DENSIMETERS: DESIGN AND OPERATION

by

Thomas Hafford Crouch

Thesis submitted to the Graduate Faculty of the

Virginia Polytechnic Institute and State University

in partial fulfillment of the requirements for the degree of

MASTER OF SCIENCE

in

Physics

APPROVED:

S. P. Almeida, ~~Chairman~~

L. B. Barnett

L. D. Roper

J. R. Vercellotti

July, 1973

Blacksburg, Virginia

ACKNOWLEDGEMENTS

The author wishes to acknowledge the help of his advisory commettee: Dr. S. P. Almeida; Dr. L. B. Barnett; Dr. L. D. Roper; and Dr. J. R. Vercellotti. The author is especially grateful to Dr. L. B. Barnett, Dr. J. R. Vercellotti, , and for their help in sample preparation and composition determination.

Extreme gratitude is extended to Dr. T. E. Leinhardt, Dr. D. W. Kupke, Dr. D. L. Deardorff, , , , , and for their kind help in designing and constructing the two instruments used in these experiments.

Finally, the author wishes to thank , his wife, for help in preparing and typing this final version and to thank her for her patience during the last four years.

TABLE OF CONTENTS

		Page
	ACKNOWLEDGEMENTS	ii
	LIST OF FIGURES	v
I.	INTRODUCTION	1
II.	METHODS OF MEASURING DENSITY	5
	A. Pycnometry	5
	B. Density Gradient Columns	6
	C. Isopycnic Temperature Method	7
	D. Hydrostatic Weighing Method	7
	E. Magnetic Densimetry	8
III.	INSTRUMENTATION	9
	A. Theory of Operation	9
	B. Glass Floats	16
	C. Solenoid Construction	19
	D. Sample Cells	22
	E. R. F. Sensing Circuit	33
	F. Optical Sensing System	37
	G. Control System	40
	H. Temperature Control	43
IV.	OPERATION	45
	A. Operational Procedures and Calibration	45
	B. Theory of Partial Specific Volume Measurements	60
	C. Partial Specific Volume Measurements of Bovine Serum Albumin in Distilled Water, $CaCl_2$, and KCl Using the R. F. Sensing Densimeter	64
	D. Partial Specific Volume Measurements of Bovine Serum Albumin in Distilled Water and Sodium Phosphate Buffer (pH 5.68), Using the Optical Sensing Densimeter	75
	E. Preferential Interactions	79
V.	CONCLUSION	106
APPENDIX A		
	Temperature Control	109

Page

APPENDIX B

Pressure Effects 111

APPENDIX C

Determination of the Extinction Coefficient of Bovine Serum Albumin 112

REFERENCES 116

VITA 118

LIST OF FIGURES

		Page
Figure 1.	Block Diagram of Densimeters	3
Figure 2.	Glass Float	11
Figure 3.	Schematic of a Solenoid	21
Figure 4.	Cross Section of the R. F. Sensing Densimeter	24
Figure 5.	Top View of Figure 4	26
Figure 6.	Cross Section of the Optical Sensing Densimeter	29
Figure 7.	Top View of Figure 6	31
Figure 8.	Schematic of the R. F. Sensing Densimeter Electronics	35
Figure 9.	Schematic of the Optical Sensing Densimeter Electronics	39
Figure 10.	Block Diagram of the Control Networks ...	42
Figure 11.	A Plot of Table I	50
Figure 12.	A Plot of Table II	53
Figure 13.	A Plot of Table III	56
Figure 14.	A Plot of Table IV	59
Figure 15.	A Plot of Table V	67
Figure 16.	A Plot of Table VI	70
Figure 17.	A Plot of Table VII	73
Figure 18.	A Plot of Table VIII	78
Figure 19.	A Plot of Table IX	82
Figure 20.	Theoretical Results of a Titration Experiment	87
Figure 21.	A Top View of Figure 20	89

Page

Figure 22. A Plot of Table XI 94

Figure 23. A Plot of Table XI 96

Figure 24. A Plot of Tables XIII and XIV 103

Figure 25. A Plot of Tables XIII and XIV 105

Figure 26. A Plot of Table XV 115

I. INTRODUCTION

The importance of accurate liquid density measurements has become more apparent in recent years. This is especially true in the areas of: molecular weight determination (by sedimentation methods);[1] studies of various effects of perturbants (salts, pH, pressure, temperature, etc.) on macromolecular partial specific volumes;[2] studies of preferential interactions among solvent components and macromolecules;[3] and determination of equilibrium constants between species in solution.[4] There are various methods of measuring densities to within several parts per million. These methods include: pycnometry, density-gradient columns, isopycnic temperature methods, hydrostatic weighing methods, a resonance frequency method, and magnetic densimetry.[4] While each method has its advantages and disadvantages, the magnetic densimeter appears to be the most versatile instrument.

Beams and Clarke[5] were the first to develop the art of magnetic densimetry. The basic principle of operation is that a float of fixed density, containing ferromagnetic material, is held at a fixed position within a liquid solution by a magnetic field. The magnitude of current required to generate this magnetic field can be directly related to solution density. A block diagram of a magnetic densimeter is shown in Figure 1.

FIGURE 1: Block diagram of both densimeters showing the various component parts.

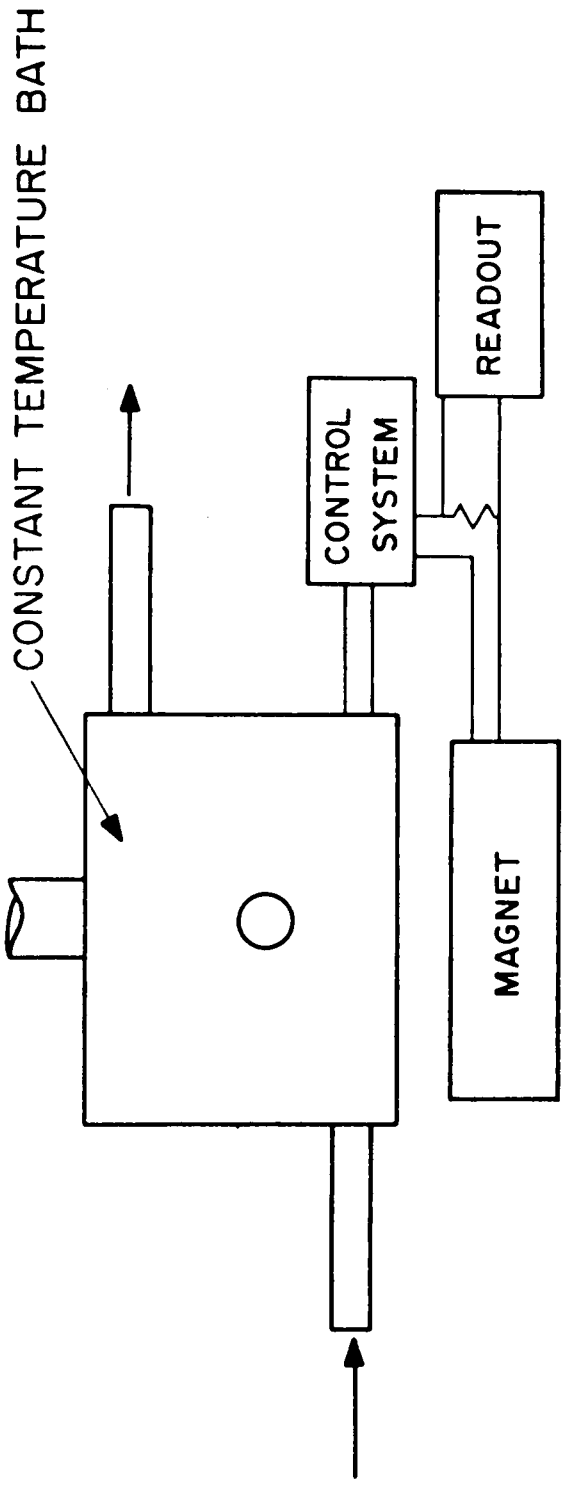
CONSTANT TEMPERATURE BATH
CONTROL SYSTEM
READOUT
MAGNET

Of primary interest is the development of a simple instrument, described above, using a simple, solid state control system. In this work two different sensing systems (each with the identical control system) are compared with respect to ease of operation, accuracy and reproducability. Calibrations with National Bureau of Standards sucrose and partial specific volume ($\overline{V}$) measurements with bovine serum albumin (BSA) are used for the basis of this comparison.

Of secondary interest is the use of these instruments in determining the effects of various solvents on the $\overline{V}$ of BSA, as well as what the future holds for this type of measurement.

II. METHODS OF MEASURING DENSITY

A. Pycnometry

A pycnometer generally consists of a glass cell, containing between 10 and 25 ml of fluid when filled, which can be easily weighed without evaporation. With this type of instrument, volumes must be kept constant to within $\pm$ .01 µl to assure accurate density measurements to within several parts per million. Liquid densities are obtained by weighing the glass cell on a balance while maintaining the cell at a constant temperature and pressure. By weighing the cell when it contains a solution of known density and when it contains a solution of unknown density, the unknown density can be determined by dividing the mass of the unknown solution by the mass of the known density solution and multiplying this quantity by the density of the known density solution.

Problems with this type of instrument are that: (1) the cell must be handled in such a manner to minimize any gain or loss of mass, (2) bubble formation introduces error into the measurement, and (3) large amounts of components are needed to get $\overline{V}$ measurements. Despite its disadvantages this method can be very useful and accurate where one is not limited to small amounts of components or small volumes.

Another instrument which also determines the mass of a fixed volume of solution has recently been developed. Here the mass of a hollow glass tube is determined by measuring its resonance frequency. By determining the period of oscillation corresponding to the resonance frequency of the tube containing one solution of unknown density and that corresponding to the resonance frequency of the tube containing one solution of known density, the unknown density can be determined. The difference in the square of the periods of oscillation is directly proportional to the difference in liquid densities. (The constant of proportionality is predetermined.) This instrument requires volumes on the order of 1 ml and does not have any of the above mentioned problems associated with it.[4]

B. Density Gradient Columns

Density gradient columns used for aqueous solutions generally consist of a column 20 cm in lenght containing a linear density gradient of two solvents such as purified kerosene and bromobenzene. Small droplets of solution (less than 1 µl) are added to the column along with droplets of standard density solutions. The solution density is determined by measuring the position of the unknown solution droplet with respect to the standard density solution droplets. The main problem with this method is the difficulty in forming and maintaining the linear

gradients. Furthermore, several theoretical questions have arisen regarding the validity of this procedure because of the aqueous-nonaqueous interface problem.[4]

C. Isopycnic Temperature Method

The isopycnic temperature method of measuring densities consists of varying the temperature of a solution whose density is to be measured until its density is identical to that of a glass float of known density. Since the densities of different solutions are determined at different temperatures, the actual $\overline{V}$ of a component cannot be determined unless it is temperature independent. This method yields densities with accuracies to ± 2 μg/ml.[4]

D. Hydrostatic Weighing Method

To determine the density of a solution using the hydrostatic weighing method, a sinker attached to an analytical balance is suspended via a fine wire into the liquid. The density of the liquid is the weight loss of the sinker divided by the sinker volume. The method has been developed so that solution volumes of less than 2 ml are required. The main obsticle to this method is the effect of surface tension on the sinker suspension wire, causing erroneous density determinations. This system does have the potential advantage of allowing titration studies.[4]

E. Magnetic Densimetry

This method is described in great detail in Section III. The principle advantages of this instrument are: (1) rapid density determination, (2) small volume requirements, (3) density measurements can be made as a function of both temperature and pressure, and (4) titration studies can be preformed. The principle disadvantage of this instrument is that bubbles tend to form on floats. Though these bubbles can usually be wiped free for normal density determinations, they cannot be wiped free durring titration studies. Thus while having many advantages, this instrument has the same drawback as most of the others--air bubbles.[4]

III. INSTRUMENTATION

A. Theory of Operation

When a magnetic densimeter is in operation, a float containing ferromagnetic material is stably supported electronically in a fluid free from the sample container walls and the meniscus. Since this float is in static equilibrium one can say that the sum of the forces on the float is zero. Thus

$$\Sigma F_x + \Sigma F_y + \Sigma F_z = 0 \qquad (1)$$

Since there are no forces lying within the x,y plane, Equation 1 reduces to

$$\Sigma F_z = 0 \qquad (2)$$

where the subscripts x,y refer to perpendicular directions within a plane normal to a vector representing the force of gravity (see Figure 2). Hence the z direction is defined to be vertical. Therefore the total F_z can be resolved into two components -- one up and one down.

These two components are the results of three forces, and, since they are co-linear, they can be added algebraically. These three forces are: buoyancy, due to difference in float and fluid density; gravitation; and magnetic forces. Of these three, only buoyancy and gravitation are directionally consistent, buoyancy being directed up and

FIGURE 2: Drawing of a typical glass float showing the directions of the forces exerted by buoyancy and the solenoid.

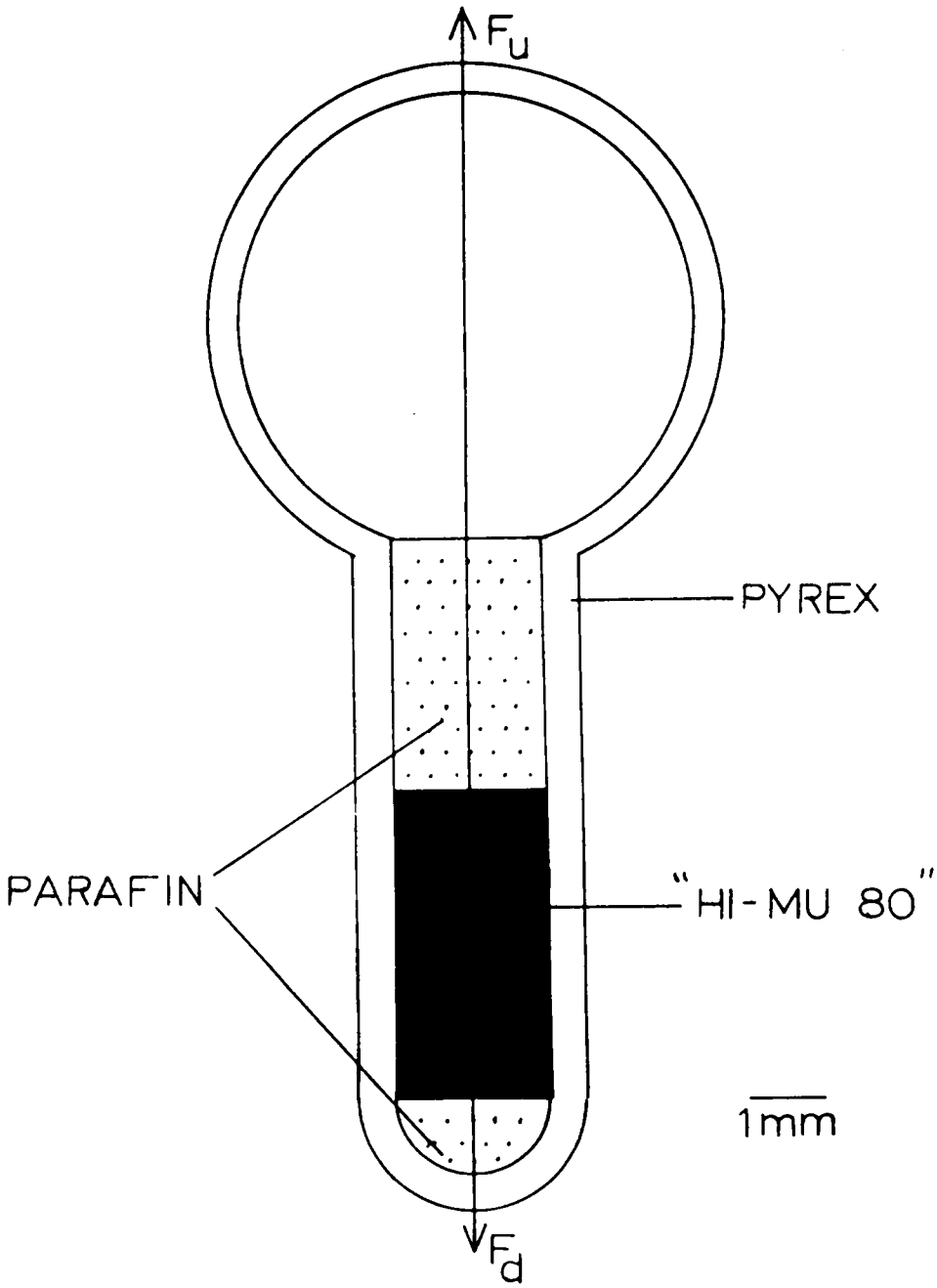
F_u
PYREX
PARAFIN
"HI-MU 80"
1mm
F_d

gravity down. However, the magnetic component may be directed in either direction by locating the support magnet above or below the float. If the float density is greater than that of the fluid, the magnetic force must be directed upward to support the float and the magnet is mounted above the sample. If, on the other hand, the float density is less than that of the solution, the float must be pulled away from the meniscus to satisfy conditions mentioned previously. In this case the magnet must be mounted beneath the sample. With both instruments used in this work, the magnet is mounted beneath the sample cell since this has the practical advantage of easy access to the sample cell allowing uncomplicated sample changing.

In a system in which the support magnet is mounted beneath the sample cell, the following derivation holds. (For a system in which the magnet is above the sample, the sign on the magnetic force component becomes negative.) In static equilibrium the upward force is equal and opposite to the downward force.

$$F_u = F_d \tag{3}$$

The upward force (F_u) on the float is given by Archemede's principle.

$$F_u = \rho_f V_B g \tag{4}$$

Where ρ_f is the fluid density, V_B is the float volume and g is the gravitational acceleration. The downward force (F_d) is the sum of gravitational and magnetic forces

$$F_d = M_B g + G(H) \tag{5}$$

where M_B is the float mass and G(H) is some function of the magnetic field. Equating equations (4) and (5)

$$\rho_f V_B g = M_B g + G(H) \tag{6}$$

rearranging

$$\rho_f = \frac{M_B}{V_B} + \frac{G(H)}{gV_B}. \tag{7}$$

Since

$$\rho_B = \frac{M_B}{V_B} \tag{8}$$

and g and V_B are constants

$$\rho_f = \rho_B + g(H) \tag{9}$$

where

$$g(H) = \frac{G(H)}{gV_B}. \tag{9a}$$

Since it is much easier and more accurate to measure current through the support electromagnet than to measure

the magnetic field directly at the float, the ferromagnetic material contained within the float must have essentially no hysteresis or "memory" of a magnetic field. The nickel alloy "Hi-Mu-80" (Carpenter Steel Company), when properly annealed, satisfies this requirement of no hysteresis. It is used in all floats. Now g(H) can be directly and consistently related to current (i) and

$$g(H) = f(i) \tag{10}$$

and equation (9) becomes

$$\rho_f = \rho_B + f(i) \tag{11}$$

where f(i) is some function of current.

The function f(i) can be further resolved. For a magnetic material, the magnetic moment M(H) is a function of magnetic field intensity H[h(H)]

$$M(H) = M_o + h(H) \tag{12}$$

where M_o is the permanent magnetic moment. The force on this magnetic material by the field H is

$$f = \vec{M}(\vec{\nabla} \cdot \vec{H}) \tag{13}$$

or in this case

$$f = \vec{M}\left(\frac{\partial \vec{H}}{\partial z}\right) \tag{14}$$

It has already been shown that H is a function of i. For most cases h(H) is a hyperbolic tangent function, and for small values of H this can be sufficiently approximated as

$$h(H) = aH \tag{15}$$

or as

$$h(H) = aH + bH^2 \tag{16}$$

since it can be shown (Section III C) that H is a linear function of i, and as experience has shown that Equation 15 provides an adequate approximation of the hyperbolic tangent functions over the regions of interest. Equation 12 becomes

$$M = M_o + Ki \tag{17}$$

where K is some constant. Now Equation 14 becomes

$$f = (M_o + Ki) \frac{\partial H}{\partial z}. \tag{18}$$

Since i is independent of z and is proportional to H, Equation 18 can become

$$f = (M_o + Ki)(\gamma i) \tag{19}$$

or by setting $M_o\gamma = b$ and $K\gamma = a$

$$f(i) = ai^2 + bi,$$

and Equation 11 becomes

$$\rho_f = \rho_B + bi + ai^2. \qquad (21)$$

Thus by measuring values of solenoid currents (i) required to stably suspend a given float in a given fixed position in solutions of known densities, and fitting the data to the above equations, one can readily calibrate a magnetic densimeter provided $|\rho_f - \rho_B|$ is small (small H).

B. Glass Floats

The basic construction of glass floats (shown in Figure 2) used with this instrument is described in great detail by senter,[2] the only difference being that floats used here were 6.5 mm across the bulb and the stems contained "Hi-Mu-80" cylinders 2 mm in diameter and 4 mm in length. (The larger "Hi-Mu-80" cylinder allowed a greater sensitivity to float change in the r.f. position sensing circuit.) Floats used with this instrument were constructed by blowing a cylindrically symmetric bulb on pieces of number 3 pyrex glass tubing (I.D. 2 mm, O.D. 3 mm) concentric with the tubing. To check for uniformity, bulbs were held at arms length and rotated slowly while gazing at some distant object through them. If the object did not appear to move, these bulbs were acceptable. Next, float stems were shortened to about 7 mm, and "Hi-Mu-80" cylinders were

inserted along with paraffin. The amount of paraffin needed was determined by observing the maximum amount which could be inserted into open floats before they sank in distilled water. Then the float stems were sealed off and glass was added to the stem bottoms until the buoys barely floated in distilled water. If necessary floats were made less dense by grinding off excess glass from this area of float stems. Floats were then heated in boiling vegetable oil and allowed to cool while rotating in a swinging bucket centrifuge. This forced slugs into float stems and symmetrically distributed paraffin inside the floats. After washing in acetone and soapy water, and rinsing with distilled water, the floats were ready for use. Though solution volumes required for the particular sample cell used with the r.f. sensing densimeters were on the order of 1.5 ml, smaller floats (with smaller slugs) could have been used. However, in such a case the marginal oscillator frequency or components would have had to be changed to give the necessary sensitivity.

Be this as it may, with the light sensing system, float size (and slug size) is unimportant as long as a sufficient magnetic moment can be induced in the slugs to pull floats to the sample cell bottom with solution present. The obvious restriction in both cases is that with sample cells mounted above a solenoid, float densities must be less than those of samples to be studied.

Slugs used with these floats must be machined from stock nickel alloy and annealed by prescribed procedure[6] in a hydrogen atmosphere. This assures totally random distribution of magnetic domains within the crystal structure prior to exposure to a magnetic field, eliminating problems with hysteresis.

The annealing process was carried out in a Lindberg "Hevi-Duty" type 167 furnace. Slugs supported in inert aluminum oxide within a ceramic boat were inserted into a large ceramic tube with one tapered end. This tube was inserted into the furnace with both ends extending outside the furnace. Hydrogen gas was passed through activated alumina into the ceramic tube and was burned as it vacated the tapered tube end. In order to maintain a temperature of 2050°F the furnace was surrounded with half-inch asbestos sheet and four-inch thick fiberglass insulation. Slugs were heated for four hours at 2050°F and were cooled to 1200°F at 500°F per hour and then to 600°F at 300°F per hour and then allowed to cool at an uncontrolled rate to room temperature. During this time hydrogen gas was allowed to pass over the slugs insuring a pure hydrogen atmosphere. All slugs were stored under acetone to isolate them from air and to remove any grease that might have been present. Floats with slugs prepared by this method gave calibration curves in reasonable agreement with Equation 21.

C. Solenoid Construction

The solenoid used with both instruments was wound on a copper spool. This spool consists of two .25 inch thick, round copper plates silver soldered to a .25 inch diameter copper rod which was about 6.5 inches between the two plates. Number 17 copper enameled wire (.04526 inches in diameter) was wound 125 turns along the spool, 50 layers deep to give a total of 6250 turns. The total amount of wire used was about 1.63 km giving a D.C. resistance of 27.52 Ω.

An approximation to the magnetic field intensity can easily be derived following Ulrich's derivation.[7] Figure 3 shows a diagram of the solenoid with the appropriate parameters defined. With the current density within the solenoid represented by j in amp/cm^2 (cgs)

$$dH = \frac{2\pi j r^2 \, dr dh}{10[(z-h)^2 + r^2]^{3/2}} \tag{22}$$

Integrating over the entire solenoid

$$H = \frac{2\pi j}{10} \int_{-b}^{+b} \int_{-d}^{+d} \frac{r^2 \, dr dh}{[(z-h)^2 + r^2]} \tag{23}$$

FIGURE 3: Schematic diagram of a solenoid showing the parameters used in Equations 22 to 25.

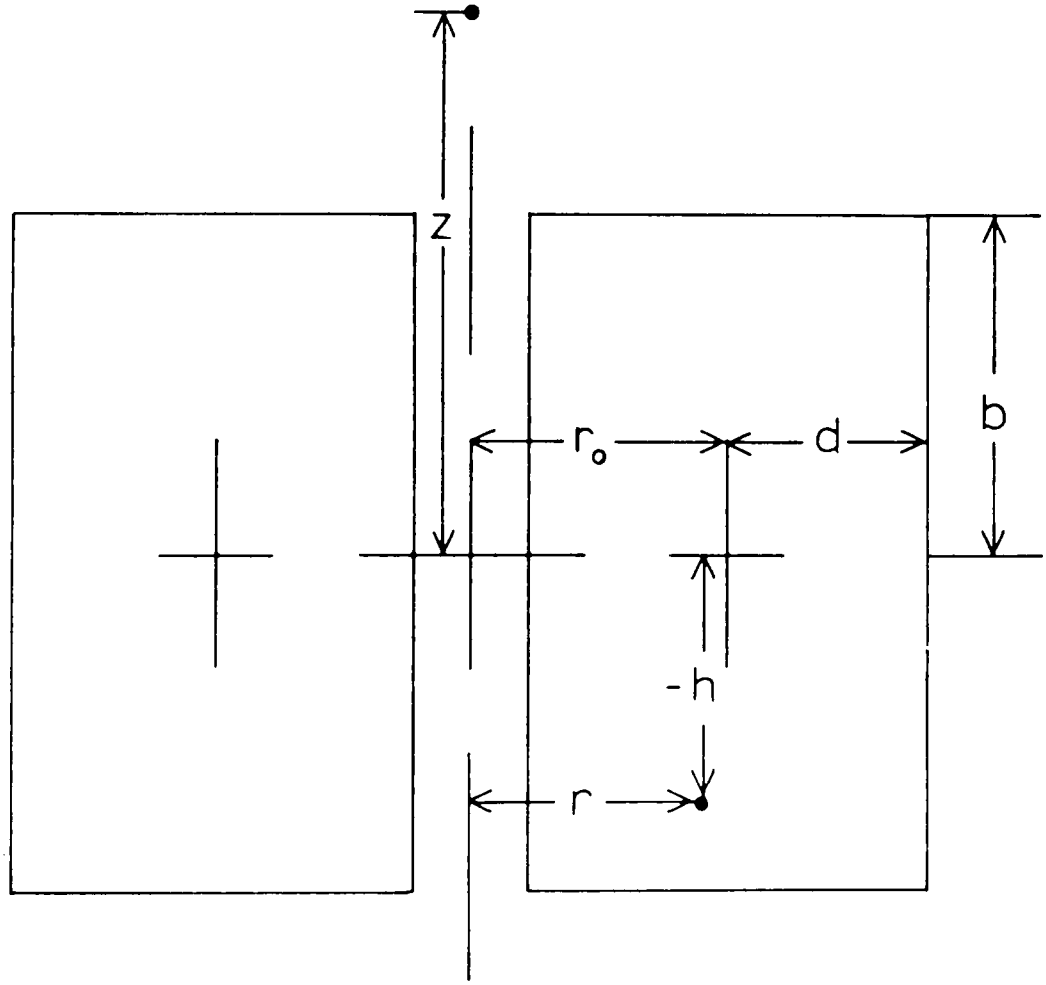
z
r_o
d
b
-h
r

Thus

$$H = \frac{2\pi j}{10}\left[(z+b)\ln\frac{r_1 + [(z+b)^2 + r_1^2]^{1/2}}{r_o + [(z+b)^2 + r_o^2]^{1/2}} - (z-b)\ln\frac{r_1 + [(z-b)^2 + r_1^2]^{1/2}}{r_o + [(z-b)^2 + r_o^2]^{1/2}}\right] \quad (24)$$

Thus

$$H = i\, f(z) \quad (25)$$

where f is a function of z similar to the bracketed relation in Equation 9. Thus H and dH/dz are both linear functions of i.

D. Sample Cells

Figure 4 shows a cross-sectional view of the sample tube and temperature bath used with the r.f. sensing densimeter. Figure 5 shows the top view. The sensing coil is mounted around the sample tube base. This coil is isolated from the temperature bath by glass since presence of water here detunes the sensing circuit. A sight tube is attached to the sample tube such that floats can be repositioned in the field of a 40X telescope with respect to crosshairs mounted within the telescope. Light for viewing the float is supplied by a light pipe aligned colinearly with the sight tube behind the sample cell. The sample

FIGURE 4: Detailed cross sectional view of the r. f. sensing densimeter showing the constant temperature bath, sensing coil, float, sighting system and solenoid.

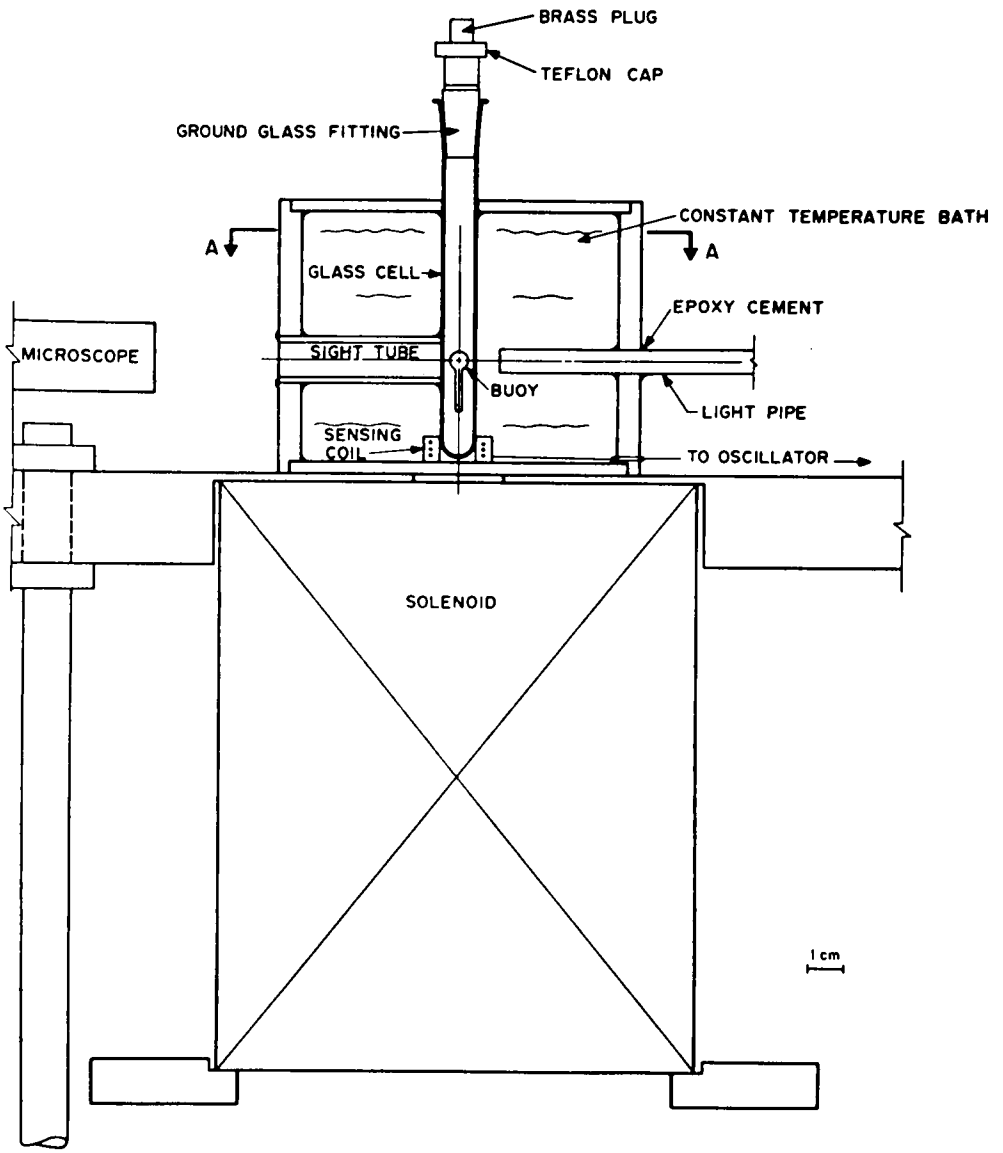
BRASS PLUG
TEFLON CAP
GROUND GLASS FITTING
CONSTANT TEMPERATURE BATH
A
A
GLASS CELL
EPOXY CEMENT
MICROSCOPE
SIGHT TUBE
BUOY
LIGHT PIPE
SENSING COIL
TO OSCILLATOR
SOLENOID
1 cm

SECTION B-B

FIGURE 5: Top view of Figure 4.

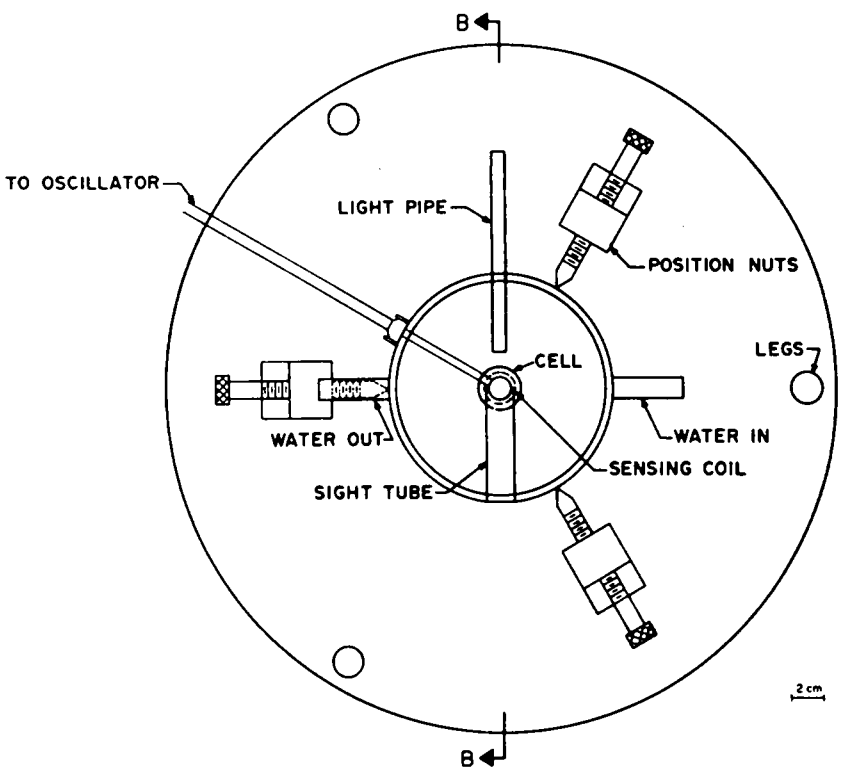
B
TO OSCILLATOR
LIGHT PIPE
POSITION NUTS
LEGS
CELL
WATER OUT
WATER IN
SENSING COIL
SIGHT TUBE
2 cm
B

SECTION A-A

tube for this sensing system is plugged with a ground glass stopper. This proved sufficient to allow a reasonable vacuum to be built up for drying the sample cell, showing evaporation need not be considered over time intervals of several hours. This particular tube has a total fluid capacity of about 5 ml (which proves invaluable for titration work) with a minimum of 1.5 ml required for one density measurement. The sample cell is mounted with sensing coil, sight tube, and light pipe in a plex-a-glass container which serves as a constant temperature bath (to measure densities to within $\pm 1 \times 10^{-6}$ gm/ml, the temperature must be maintained to within $\pm .005°C$, see Appendix A). Water from a temperature controller is pumped in at the base of the temperature bath and out at the top.

Figures 6 and 7 show the temperature bath and sample cell used with the optical sensing densimeter. The sample cell is coated with paint to cut out stray light. Four brass tubes are mounted at right angles in a plane where the top of a float will rest when the float is suspended. Two colinear tubes are used for a light source and light sensing diode, and the other two colinear tubes are used for sighting the float and for a light source to illuminate the telescope field. The outer shell of the temperature bath is brass with the brass tubes soldered in place. The top is .25 inch plex-a-glass painted black and epoxyed

FIGURE 6: Cross sectional view of the constant temperature bath for the optical sensing densimeter. The solenoid and solenoid support are identical to Figures 4 and 5. The outside diameter of the bath is three inches.

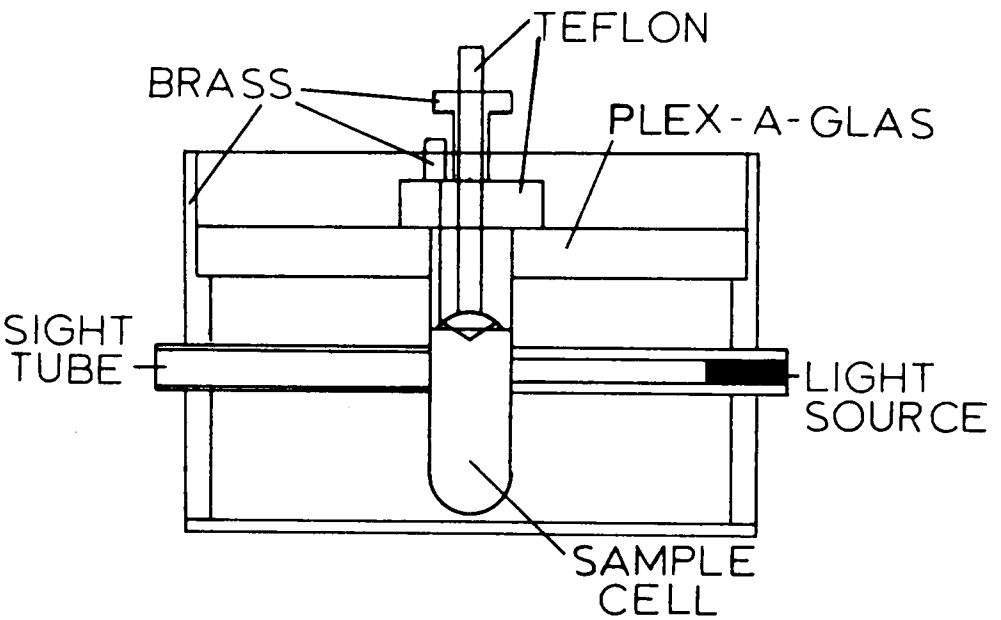
TEFLON
BRASS
PLEX-A-GLAS
SIGHT TUBE
LIGHT SOURCE
SAMPLE CELL

FIGURE 7: Top view of the constant temperature bath for the optical sensing densimeter (top view of Figure 6). The outside diameter of the bath is three inches.

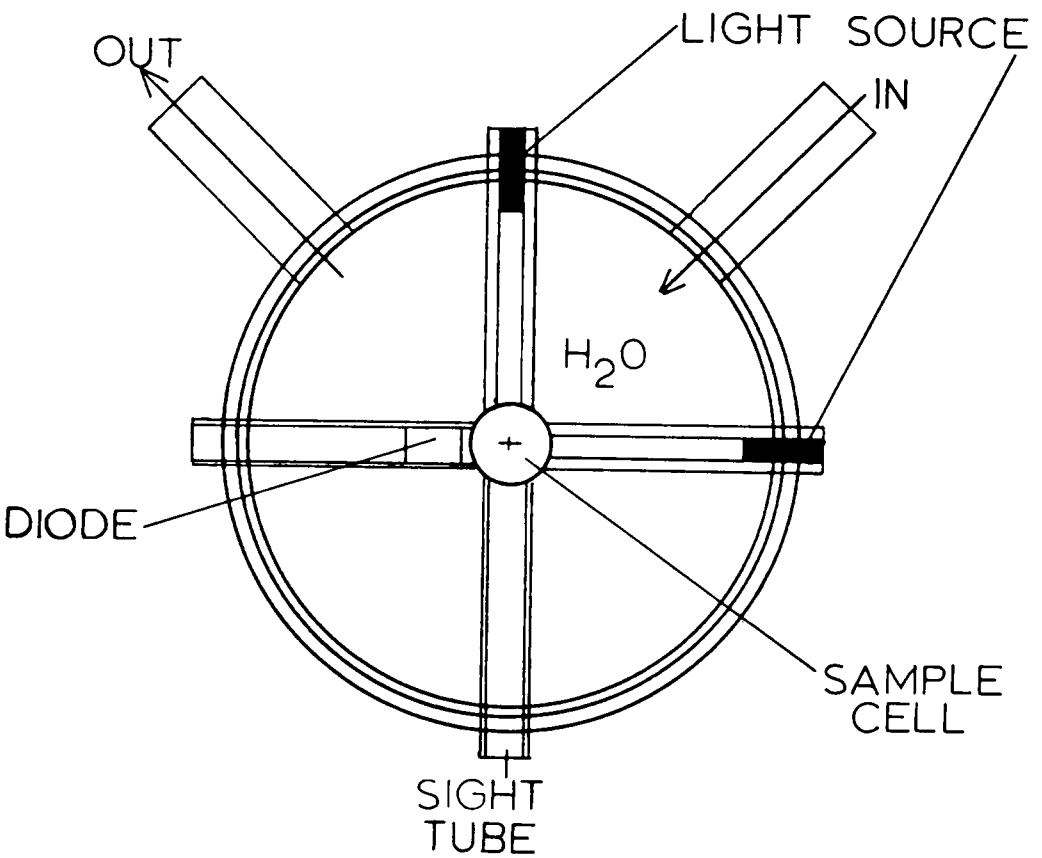
OUT
LIGHT SOURCE
IN
H_2O
DIODE
SAMPLE CELL
SIGHT TUBE

in place. The sample cell is stoppered with a teflon plug with .002 inch oversize ridges to assure a good seal. In this top a teflon rod is mounted to help remove bubbles from floats and a pinhole is used for sample induction. A minimum of 1.2 ml of solution is required for a density determination, while by adjusting the teflon plug a maximum fluid content of 2.0 ml can be attained.

One of the major problems with both of these two magnetic densimeters as well as with others is the formation of bubbles on floats. This situation is usually brought about by air dissolved in solutions to be studied, splashing of solution on introduction to the cell, and surface tension. The overall effect is the reduction of float density and erroneous density readings. Methods for purging the float of bubbles include dropping powdered teflon on the float (and "sweeping" it clean) and sweeping the float with a thin plastic or teflon rod. However, this type of procedure is detrimental to titration studies since some fluid is removed. Usually if samples are introduced slowly after being warmed slightly above cell temperature, bubbles can be kept to a minimum. Another preventive method appears to be adding a side arm to the sample cell bottom with number 2 glass tubing to form a U tube. Addition of the sample through the small tube allows bubbles to form in a separate chamber from the float, leaving only the

property of surface tension to be reckoned with in the large chamber. By simply inserting a fine glass or plastic probe into the cell and puncturing the bubble on top of the float (these bubbles always result from surface tension) this problem can be minimized.

E. R.F. Sensing Circuit

To be capable of sensing float positions with an r.f. coil a sensitive marginal oscillator is needed. The one chosen for this instrument is a transistor analog of a tuned plate-tuned grid oscillator with slight variations. The basic design is shown in Figure 8. Feedback necessary for oscillation is accomplished through internal capacitance of the FET (field effect transistor). Thus with both tank (L-C) circuits tuned to (resonating at) the same frequency, maximum oscillation occurs. However, as the tank circuit (a capacitator and inductor in parallel) in the gate circuit becomes detuned by a change of circuit parameters (capacitance or inductance), the amplitude of oscillation decreases. In general, components with higher quality factors (Q's) make the output signal amplitude more sensitive to component change. (Higher Q's are generally a result of low D.C. resistance.) Though the output signal between the drain and ground is larger and shows greater voltage change per given parameter change, impedence matching with later stages becomes a problem, and the tank

FIGURE 8: Schematic diagram of the r. f. sensing densimeter electronics.

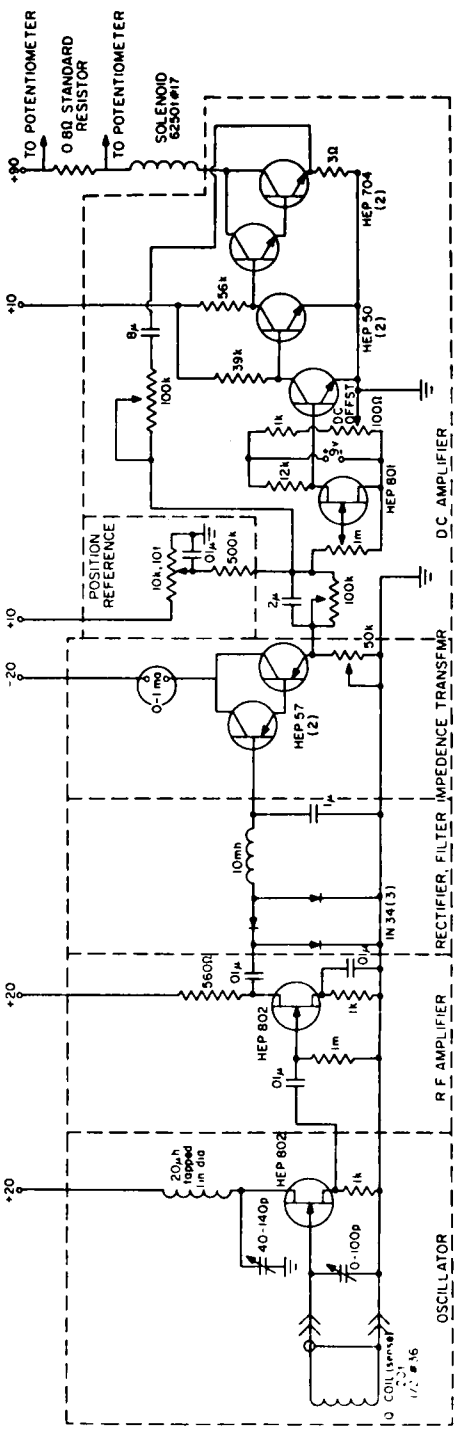
TO POTENTIOMETER
0.8Ω STANDARD RESISTOR
TO POTENTIOMETER
SOLENOID 62501#17
+90
+10
+10
-20
+20
+20
3Ω
HEP 704 (2)
56k
HEP 50 (2)
8μ
39k
100k
DC OFFST
100Ω
1k
9v
12k
HEP 801
1m
POSITION REFERENCE
10k, 10t
.01μ
500k
2μ
100k
50k
0-1 ma
HEP 57 (2)
1μ
10mh
IN 34 (3)
560Ω
.01μ
HEP 802
1k
1m
.01μ
HEP 802
20μh tapped 1 in dia
40-140p
0-100p
1k
OSCILLATOR
RF AMPLIFIER
RECTIFIER, FILTER
IMPEDENCE TRANSFMR
DC AMPLIFIER

circuit can easily become detuned by a change in parameters between this point and the next stage. Thus the output signal is taken between the source of the FET and ground. At this point the output impedence is low and component variations in following stages, while having some effect on maximum oscillation amplitude due to bias, have little effect on the tuning. The output of the marginal oscillator is amplified by a simple FET r.f. amplifier, rectified by a full-wave diode bridge, and filtered by an L-C filter. At this point a transistor configuration called a darlington pair serves to further filter the signal, lower the impedence and provide a current amplifier for a 0-1 ma meter which is used to determine if the oscillator is properly tuned. This is the float position sensing circuit (see Figure 8). The sensing circuit operates as follows. Coil L_1 (20 turns, #36 wire .5 inch diameter) is positioned at the sample cell base as shown in Figure 4. The oscillator is tuned by adjusting either C_1 (0-100 pf) or C_2 (40-140 pf) or both so that as the float settles, the output signal amplitude decreases and as the float rises, the output signal increases. (As the float moves up and down, the ferromagnetic slug inside changes the inductance of L_1 and tunes or detunes the gate tank circuit, changing oscillator output voltage amplitude.)

This amplitude is then converted to a direct current signal. To drive the solenoid with this signal a simple analog device is used.

F. Optical Sensing System

Figure 9 shows a schematic of the optical sensing system. This consists of essentially two emitter follower transistor configurations, with the first of the configurations consisting of a photo diode instead of an ordinary NPN transistor. As the float rises in the solution it interrupts a light beam which raises the voltage at the base of the HEP 57. The second emitter follower produces approximately the same voltage at the amplifier input with a lower output impedence. This voltage is used by essentially the same analog control circuit as the r.f. sensing system to control float positions.

This system proved much more stable than the r.f. sensing unit. This is probably because of power supply instability. The supply used with the r.f. sensing circuit was introducing 60 cycle modulation into the oscillator circuit, or 60 cycle pickup in the gate circuit of the oscillator. Be this as it may, any electrical perturbation in the 110 volt A.C. current could be seen reflected in float movement within the r.f. system. Since the optical system uses direct current and is powered by one

FIGURE 9: Schematic diagram of the optical sensing densimeter electronics.

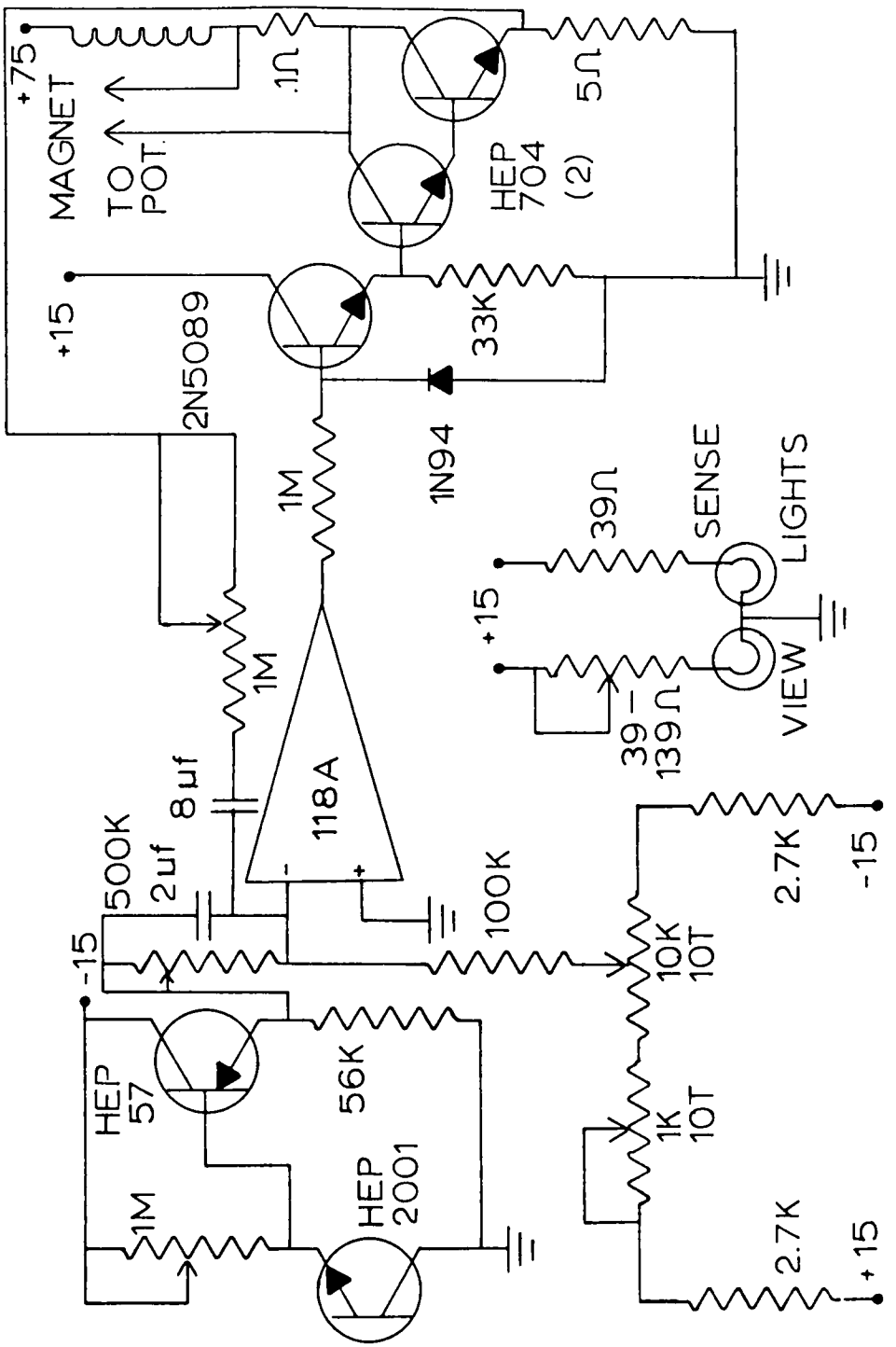
+75
MAGNET
TO POT.
.1Ω
5Ω
HEP 704 (2)
+15
2N5089
33K
1N94
1M
39Ω
SENSE
LIGHTS
+15
VIEW
39 – 139Ω
1M
8μf
118A
500K
2uf
-15
100K
10K 10T
2.7K
-15
HEP 57
56K
1K 10T
HEP 2001
1M
2.7K
+15

high-quality power supply, transients tend to be suppressed. Furthermore transients are averaged out in the light bulb used as the light source. Hence the optical system is more trouble free than the r.f. sensing system.

G. Control System

A schematic diagram of the control system is shown in Figure 10. It consists essentially of an operational amplifier followed by a current amplifier (this is essentially one amplifier). When coupled with one of the sensing systems, this circuit functions by regulating currents in the solenoid so as to hold a float in a constant position. Looking at Figure 10 one sees a simplified version of the control system. This configuration allows one to calculate the solenoid current as a function of voltage from the sensing circuit. This function is

$$e_o = i_o R_4 \simeq -(R_1 C_1 \frac{de_{in}}{dt} + \frac{1}{C_2} \int \frac{e_{in}}{R_2} + \frac{e_{ref}}{R_3} dt). \qquad (26)$$

This equation is arrived at in the following manner. The amplifier inverting input (-) in Figure 10 is a summing point for the amplifier. The feedback network consisting of R_1 and C_2 serves to integrate the D.C. voltage components e_{in} and e_{ref}, since no D.C. current i can pass capacitator C_2. Any change in i_{in} is passed through both

FIGURE 10: Block diagram of the control network showing values used in Equation 26.

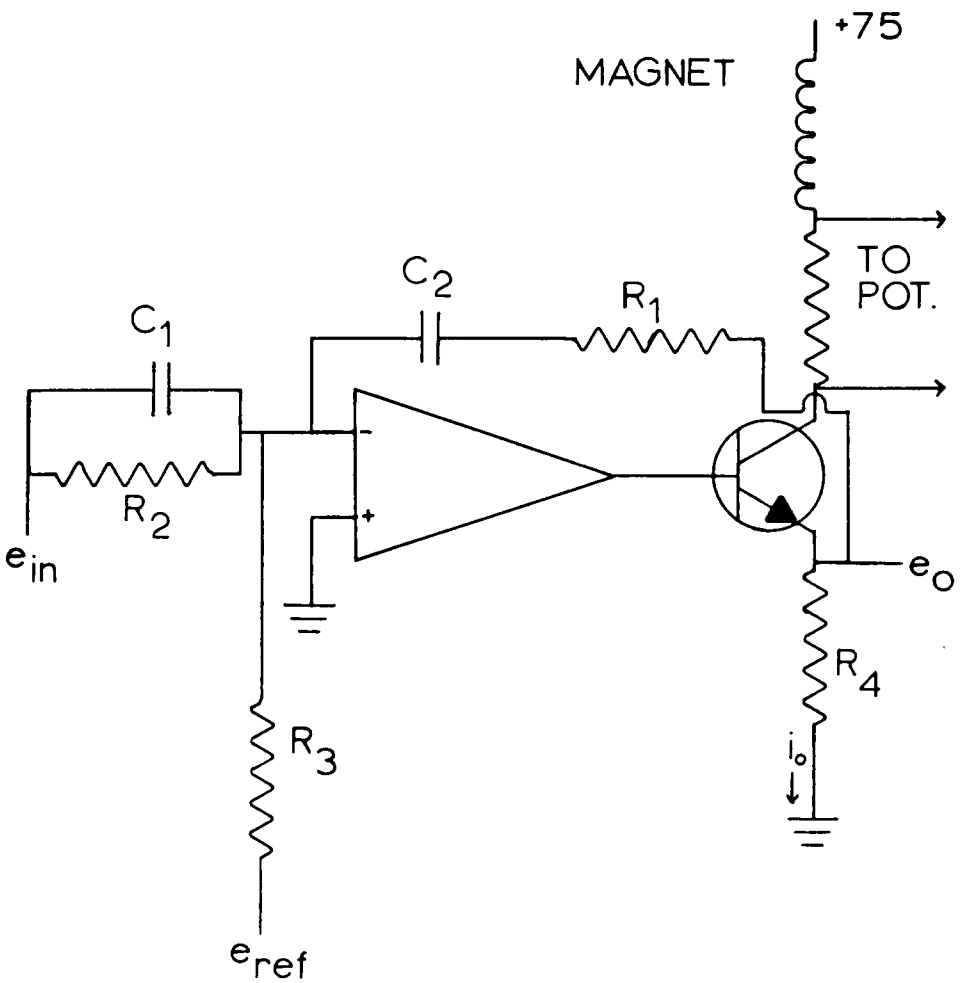
+75
MAGNET
TO
POT.
C2
R1
C1
R2
ein
eo
R4
R3
io
eref

C_1 and C_2 but is retarded by R_1. Upon summing all incoming currents, one attains equation (26), meaning this circuit not only corrects for changes in float position (distance) but also for rate of change of float position (velocity, the first derivative of distance with respect to time).

To measure i_o, a small standard resistor of approximately .1 Ω (optical sensing) or .8 Ω (r.f. sensing) is placed in series with the solenoid in the collector circuit of the darlington pair in Figure 8. By measuring voltage across this resistor with a Leeds and Northrop K-3 potentiometer, one can know the currents through it. Though the exact resistance of the standard resistor is not known accurately, the only requirement is that its resistance remain constant since the instrument is calibrated with solutions of known densities.

H. Temperature Control

As is shown in Appendix A, in order to measure aqueous solution densities to within $\pm 10^{-6}$ gm/ml, the sample temperature must be kept constant to within ±.005°C. To attain this goal a Haake model FT temperature controller was tried. This instrument proved unsatisfactory as shipped from the manufacturer. Therefore, several modifications were made which increased the sensitivity of the regulation; however, there was no way of controlling the accuracy of this instrument since the resistance bridge in the

temperature sensing unit proved susceptible to room temperature changes making it almost impossible to maintain a given temperature to within ±.2°C over a period of several hours. Upon replacing the platinum resistance thermometer bridge with a contact thermoregulator the temperature could be controlled to within ±.015°C with a period of oscillation of approximately 10 seconds in the control bath itself. This small, rapid oscillation is probably averaged out by the glass barrier between the solution to be measured and the constant temperature bath since no density oscillations can be observed within that period. Hence this method of temperature control proved quite adequate.

IV. OPERATION

A. Operational Procedures and Calibration

Samples are introduced into the cell by means of a gas lock syringe and needle. Samples are added drop by drop in such a manner that most drops fall directly on top of the float in the r.f. sensing system. This is to prevent bubbles from forming when floats are separated from the meniscus and keeps bubbles from forming around float necks. Usually during this procedure, after fluid depth is sufficient to cover a given float, the controls are adjusted so that the float is immediately pulled to and remains on the cell bottom. After the last drop of sample is introduced the float is released and allowed to come to an equilibrium position where the top is aligned with the crosshairs of a 40X telescope. Within several minutes the float position stabilizes and a reading is taken from the Leeds and Northrup K-3 potentiometer. With the optical sensing system, samples are injected at the cell bottom while holding a float down with the teflon rod mounted in the cell top. If bubbles are detected on a float, this teflon rod is used to both wipe bubbles off float tops and jar any free that are under float necks. Again the float is aligned with the telescope crosshairs and a voltage reading is taken. Since, as mentioned earlier, it is next

to impossible to theoretically predict a voltage reading across the standard resistor versus density curve to six decimal places, sucrose solutions of known densities are used to calibrate the instrument.

The sucrose used for calibrating this densimeter was purchased from the National Bureau of Standards, Gaithersburg, Maryland (Standard Sample #17, Lot #6340). And the density tables published by the Bureau[9] were used as a reference. Each sample was introduced into the cell as described above. Two different floats were used in this work: float I and float II. Their calibration data are shown in Tables I and II respectively.

Each sample was prepared by weighing out a given amount and weighing the amount of quartz glass distilled water added to the sucrose. All weighings were carried out on a Mettler H-16 balance. Though the balance is readable to ±10 μg, the readings differed from one end of the scale to the other by a maximum of ±300 μg; thus all weighings are to within ±300 μg. The sucrose concentration error involved is computed as follows where M_1 is the sucrose mass and M_2 is the total solution mass.

$$C = \frac{M_1 \pm .0003}{M_2 \pm .0006} = \frac{M_1 \pm .0003}{M_2} \left(\frac{1}{1 \pm \frac{.0006}{M_2}} \right) \qquad (27)$$

expanding

$$C = \frac{M_1 \pm .0003}{M_2}\left[1 \pm \frac{.0006}{M_2}\right] \tag{28}$$

$$C = \frac{M_1}{M_2} \pm \frac{.0003}{M_2} \pm \frac{M_1}{M_2}(.0006) \tag{29}$$

$$C = \frac{M_1}{M_2} \pm \frac{(2M_1 + 1)(.0003)}{M_2} \tag{30}$$

Since M_1 is on the order of 1 gm maximum and M_2 is on the order of 30 gm,

$$C \simeq \frac{M_1}{M_2} \pm .00003 \tag{31}$$

This gives a density error of $\pm 12X10^{-6}$ gm/ml in the standard solutions. Thus the accuracy of this instrument is limited to $\pm 12X10^{-6}$ gm/ml while its precision or reproducibility is limited to $\pm 2X10^{-6}$ gm/ml due to temperature control errors of $\pm .01°C$ (see Appendix A). Tables I and II show calibration curves for floats I and II respectively with the r.f. sensing densimeter. Float I was used for $\bar{V}$ measurements with this instrument while float II was used for titration studies with metal ligands. In these tables it can be seen that Equation 21 is adequate to describe density as a function of reading over the domain of readings listed in Tables I and II. The values in Tables I and II are plotted in Figures 11 and 12 respectively. Tables III and IV give calibration data for float II with the optical sensing

TABLE I

Calibration Curve for Float I
(r.f. Sensing Densimeter)

Reading V (Volts)	Known Density ρ_o (gm/ml)	Calculated Density ρ (gm/ml)	Difference $(\rho-\rho_o)X10^{-6}$ $(gm/ml)X10^{-6}$
.13945	0.998234	.998236	+2
.20556	1.001268	1.001252	-16
.21385	1.001708	1.001714	+6
.23764	1.003127	1.003135	+8
.33626	1.010618	1.010619	+1

$$\rho = 0.13200\ V^2 + 0.00011\ V + 0.99565$$

FIGURE 11: A plot of the values in Table I. Density is plotted as a function of densimeter reading.

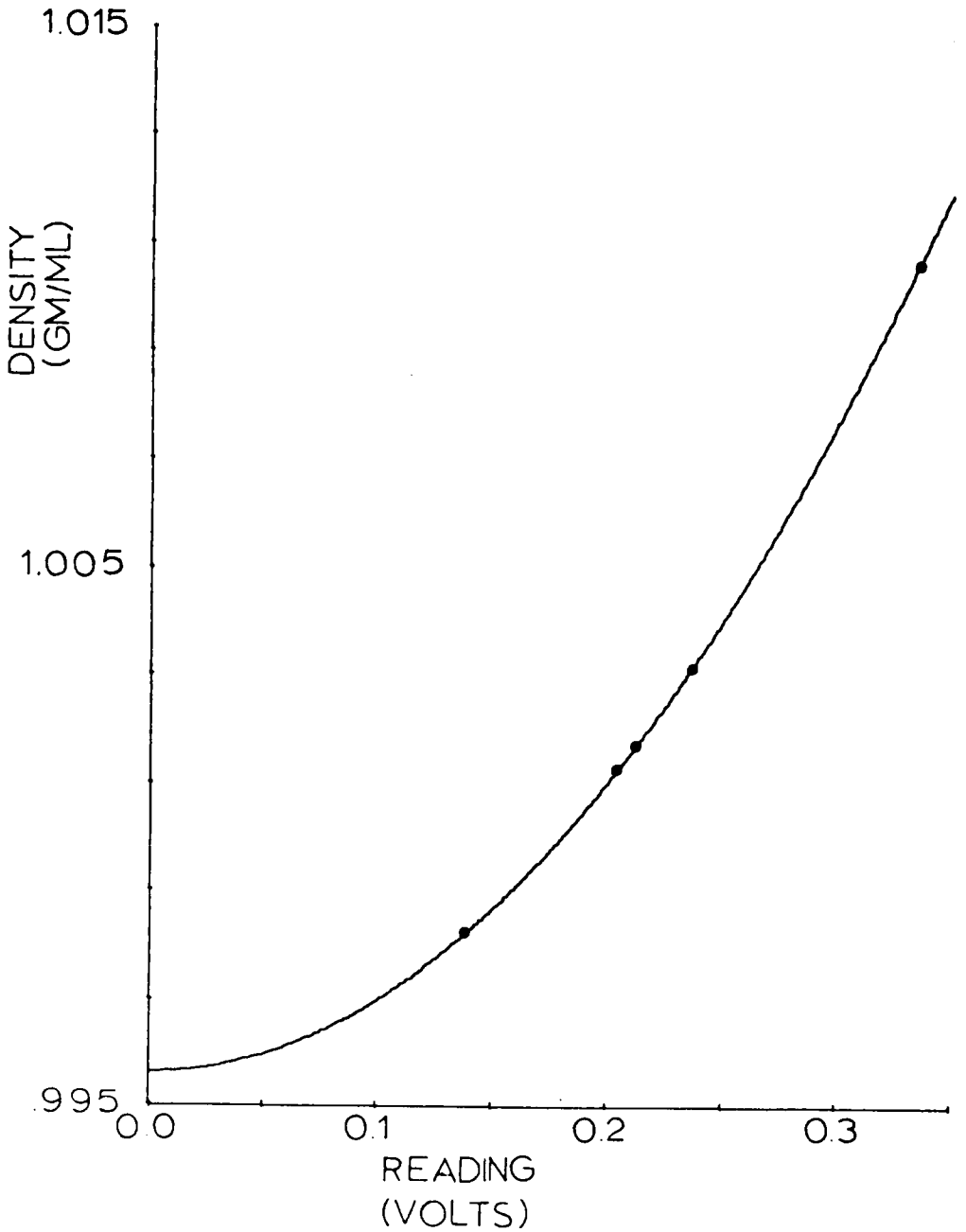
1.015
1.005
.995
DENSITY
(GM/ML)
0.0
0.1
0.2
0.3
READING
(VOLTS)

TABLE II

Calibration Curve for Float II
(r.f. Sensing Densimeter)

Reading V (Volts)	Known Density ρ_o (gm/ml)	Calculated Density ρ (gm/ml)	Difference $(\rho-\rho_o)X10^{-6}$ (gm/ml)$X10^{-6}$
.16287	.998234	.998227	-7
.19904	.999568	.999594	+27
.22417	1.000739	1.000713	-26
.25855	1.002462	1.002467	+5
.27600	1.003455	1.003456	+1

$$\rho = 0.109353\ V^2 - .001769\ V + .995614$$

FIGURE 12: A plot of the values in Table II. Density is plotted as a function of densimeter reading.

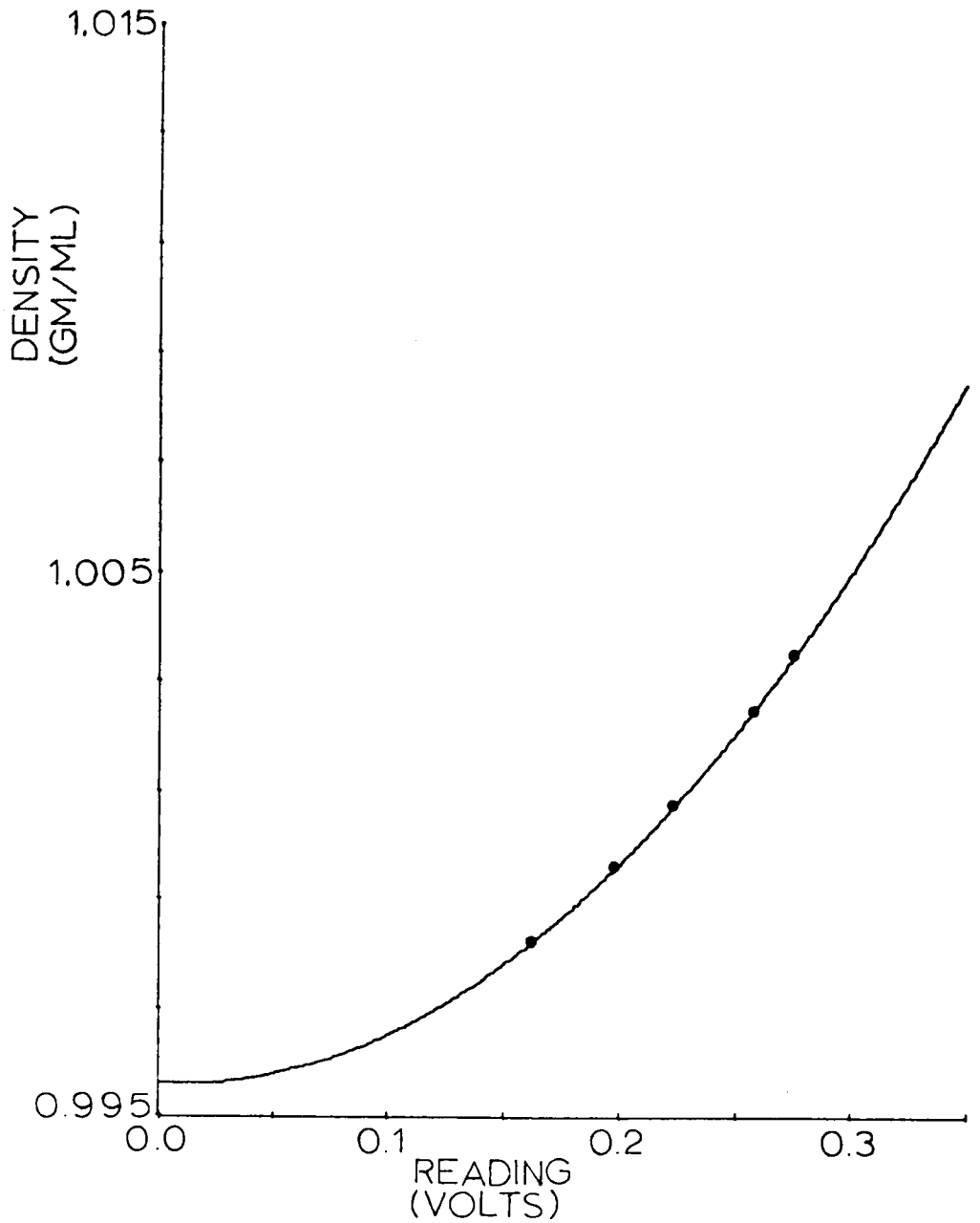
1.015
1.005
0.995
DENSITY
(GM/ML)
0.0
0.1
0.2
0.3
READING
(VOLTS)

TABLE III

Calibration Curve for Float II
(Optical Sensing Densimeter)

Reading V (Volts)	Known Density ρ_o (gm/ml)	Calculated Density ρ (gm/ml)	Difference $(\rho-\rho_o)X10^{-6}$ $(gm/ml)X10^{-6}$
.017739	.998234	.998236	+2
.024266	1.000493	1.000475	-18
.028061	1.002084	1.002103	+19
.032625	1.004372	1.004380	+8
.033640	1.004935	1.004933	-2
.040141	1.008898	1.008886	-12
.048587	1.015069	1.015073	+4

$$\rho = .08340307\ V^2 - .00073783\ V + .99574276$$

FIGURE 13: A plot of the values in Table III. Density is plotted as a function of densimeter reading.

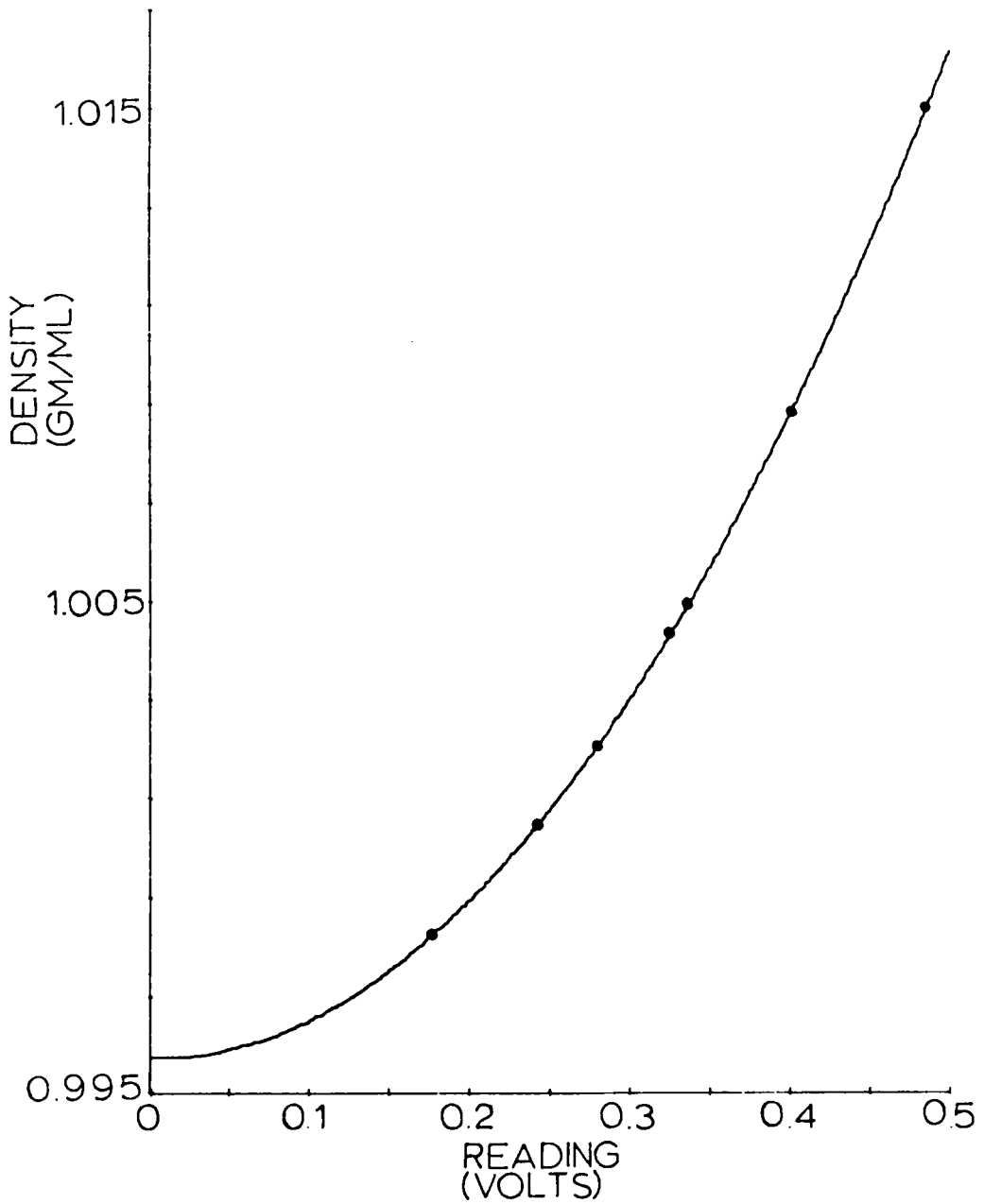
1.015
1.005
0.995
DENSITY
(GM/ML)
0
0.1
0.2
0.3
0.4
0.5
READING
(VOLTS)

TABLE IV

Calibration Curve for Float II
(Optical Sensing Densimeter)

Reading V (Volts)	Known Density ρ_o (gm/ml)	Calculated Density ρ (gm/ml)	Difference $(\rho-\rho_o)X10^{-6}$ (gm/ml)$X10^{-6}$
.017607	.998234	.998241	+7
.029536	1.002737	1.002722	-15
.037290	1.006868	1.006849	-19
.042676	1.010249	1.010278	+29
.047595	1.013792	1.013813	+21
.051848	1.017203	1.017180	-17

$$\rho = .079525\ V^2 + .00007419\ V + .995763$$

FIGURE 14: A plot of the values in Table IV. Density is plotted as a function of densimeter reading.

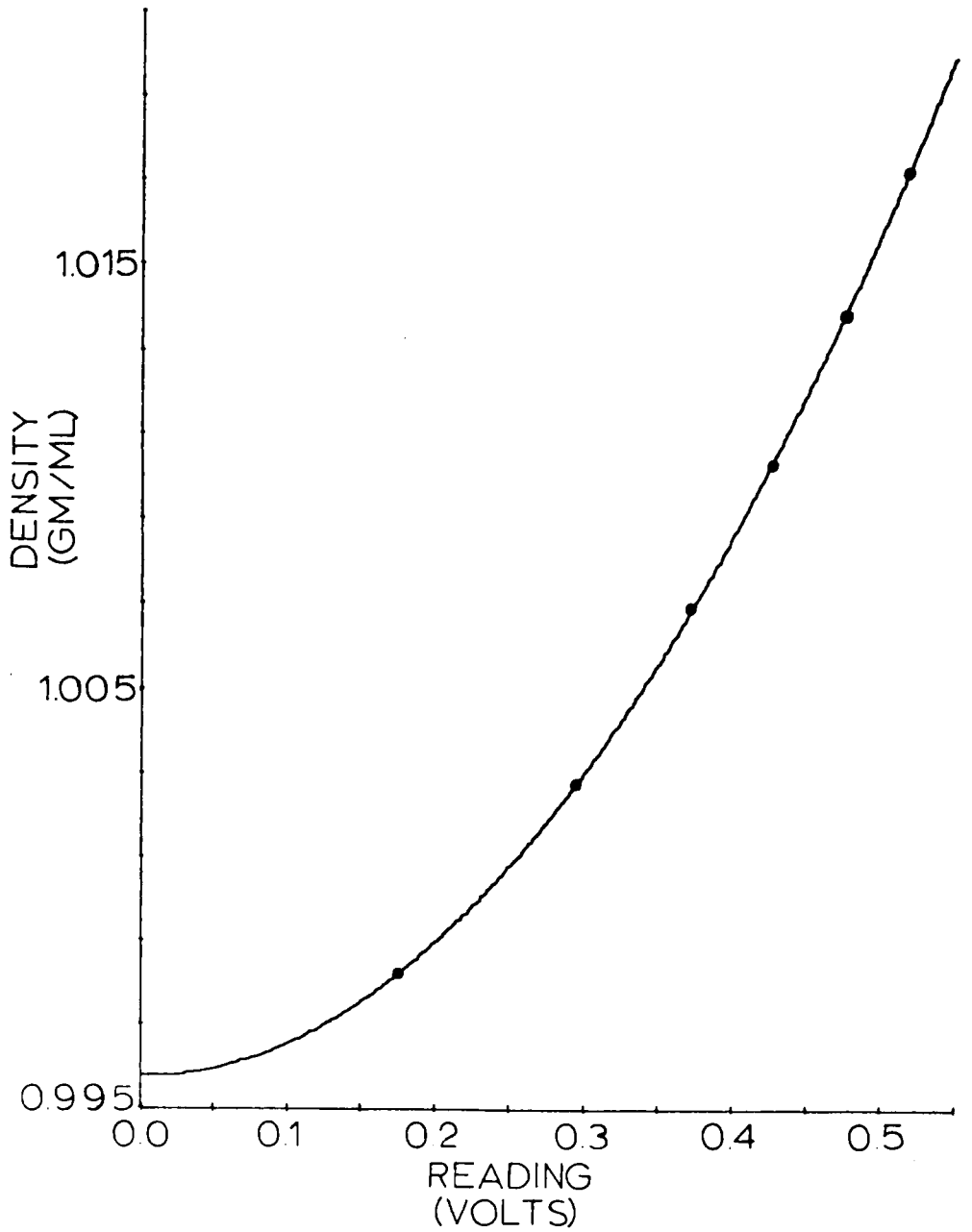
1.015
1.005
0.995
DENSITY
(GM/ML)
0.0
0.1
0.2
0.3
0.4
0.5
READING
(VOLTS)

densimeter. The values in these tables are plotted in Figures 13 and 14 respectively. The difference arises from the fact that data in Table III was taken using distilled water stored in nalgene containers, while the data in Table IV was taken using distilled water stored in pyrex. The pyrex distilled water gave the same reading in both data sets. The difference in curves is due to plasticizers dissolved in water used for sucrose standards in Calibration Curve III. Curve IV shows considerable deviation from Equation 21, as compared to Curve III. This is possibly because the domain of readings exceeds that for which the approximations leading to Equation 21 are valid or inaccurate standards. Nonetheless, over the domain of interest (for $\bar{V}$ measurements) Equation 21 is quite adequate.

B. Theory of Partial Specific Volume Measurements

The theory of partial specific volume ($\bar{V}$) measurements is well discussed in the literature.[4,10] Where density measurements are involved one uses the relation

$$\bar{V}_i = \frac{1}{\rho_o}\left[1 - \left(\frac{\partial \rho}{\partial c_i}\right)_{c=o}\right]_{m_i,\ T,\ P} \qquad (32)$$

where ρ_o is the solvent density and c_i is the concentration (gm/ml) of the ith component. This equation may be derived in the following manner.[4] Realizing that $\bar{V}_i$ of the ith

solution component is

$$\bar{V}_i \equiv \frac{\partial V}{\partial m_i} \tag{33}$$

the total volume V of a given solution becomes

$$V = \sum_{i=1}^{N} \bar{V}_i m_i \tag{34}$$

recalling that density can be defined as

$$\rho \equiv \sum_{i=1}^{N} c_i . \tag{35}$$

Differentiating Equation 35 with respect to the second component

$$\left(\frac{\partial \rho}{\partial c_2}\right)_{m_j} = \frac{\left(\sum_{i=1}^{N} \partial c_i\right)}{\partial c_2} = 1 + \sum_{j \neq 2}^{N} \frac{\partial c_j}{\partial c_2} \tag{36}$$

recalling the definition of c_2

$$\left(\frac{\partial \rho}{\partial c_2}\right)_{m_j} = 1 + \sum_{j \neq 2}^{N} \frac{\partial c_j}{\partial (m_2/V)} \tag{37}$$

applying the chain rule

$$\left(\frac{\partial \rho}{\partial c_2}\right)_{m_j} = 1 + \sum_{j \neq 2}^{N} \left(\frac{\partial c_j}{\partial m_2} \frac{\partial m_2}{\partial (m_2/V)}\right) \tag{38}$$

$$\left(\frac{\partial \rho}{\partial c_2}\right)_{m_j} = 1 + \sum_{j\neq 2}^{N} \left[\frac{\partial c_j}{m_2} \quad \frac{\partial (m_2/V)}{\partial m_2}\right] \tag{39}$$

$$\left(\frac{\partial \rho}{\partial c_2}\right)_{m_j} = 1 + \sum_{j\neq 2}^{N} \frac{\partial c_j/\partial m_2}{\left(\frac{V - m_2 \partial V/\partial m_2}{V}\right)} \tag{40}$$

substituting equation (33)

$$\left(\frac{\partial \rho}{\partial c_2}\right)_{m_j} = 1 + \sum_{j\neq 2}^{N} \frac{\partial c_j/\partial m_2}{\frac{V - m_2 \overline{V}_2}{V}} \tag{41}$$

$$\left(\frac{\partial \rho}{\partial c_2}\right)_{m_j} = 1 + \sum_{j\neq 2}^{N} \frac{(\partial c_j/\partial m_2)V}{1 - c_2 \overline{V}_2} \tag{42}$$

$$\left(\frac{\partial \rho}{\partial c_2}\right)_{m_j} = 1 + \frac{V}{1 - c_2 \overline{V}_2} \sum_{j\neq 2}^{N} \frac{\partial c_j}{\partial m_2} \tag{43}$$

$$\sum_{j\neq 2}^{N} \frac{\partial c_j}{\partial m_2} = \sum_{j\neq 2}^{N} \frac{\partial (m_j/V)}{\partial m_2} = - \sum_{j\neq 2}^{N} \frac{m_j \frac{\partial V}{\partial c_2}}{V} = \tag{44}$$

$$- \frac{\overline{V}_2}{V} \left(\frac{m_2}{V} - \frac{m_2}{V} + \sum_{j\neq 2}^{N} \frac{m_j}{V}\right)$$

$$\sum_{j\neq 2}^{N} \frac{\partial c_j}{\partial m_2} = \frac{\overline{V}_2}{V} (\rho - c_2). \tag{45}$$

Thus

$$\left(\frac{\partial \rho}{\partial c_2}\right)_{m_j} = 1 - \frac{V}{1 - c_2\overline{V}_2}\left(\frac{\overline{V}_2(\rho - c_2)}{V}\right) \tag{46}$$

$$\left(\frac{\partial \rho}{\partial c_2}\right)_{m_j} = \frac{1 - \overline{V}_2\rho}{1 - c_2\overline{V}_2}. \tag{47}$$

Rearranging

$$\overline{V}_2 = \frac{1 - \left(\frac{\partial \rho}{\partial c_2}\right)_{m_j}}{\rho - c_2\left(\frac{\partial \rho}{\partial c_2}\right)_{m_j}} \tag{48}$$

in the limit as c_2 approaches zero or if ρ is a linear function of c_2

$$\overline{V}_2 = \frac{1}{\rho_o}\left(1 - \left(\frac{\partial \rho}{\partial c_2}\Big|_{c_2=o}\right)_{m_j,T,P}\right) \tag{49}$$

Thus by plotting ρ as a function of c_2 for small second component concentrations $\overline{V}_2$ can be determined. For multi-component systems the same procedure is followed since the

apparent $\bar{V}_i(\phi_i)$ can be shown equivalent to the actual $\bar{V}_i$ at vanishing c_i.

$$\phi = \frac{\partial V}{\partial m_i} = \frac{\partial \Sigma m_j \bar{V}_j}{\partial m_i} = V_i + m_i \left(\frac{\partial \bar{V}_i}{\partial m_i}\right)_{m_j} \qquad (50)$$

Thus as m_i approaches zero $_i = \bar{V}_i$. Thus the equation

$$\bar{V}_i = \frac{1}{\rho_o}\left[1 - \left(\frac{\partial \rho}{\partial c_i}\Big|_{c_i=o}\right)_{m_j,T,P}\right] \qquad (51)$$

gives the actual $\bar{V}$.

C. Partial Specific Volume Measurements of Bovine Serum Albumin in Distilled Water, $CaCl_2$, and KCl Using the R.F. Sensing Densimeter

As was shown above, $\bar{V}$'s of proteins can be determined by measuring densities of several dilutions of a given protein concentration by its solvent. To prepare the samples on BSA (Bovine Serum Albumin Sigma Fraction V, powder lot #4503, 95% pure) was dialysed against distilled water, another against a $CaCl_2$ solution and another against a KCl solution. Each dialysis was performed in an Amicon (#402) ultra filtration system using a UM-10 membrane. After dialysis each solution was diluted with its solvent solution. The BSA concentrations were determined spectrophotometrically using a pre-determined extinction coefficient of

TABLE V

$\bar{V}$ of Albumin in Distilled Water

Albumin Concentration (C_2) (gm/ml)	Density ρ_o (gm/ml)	Calculated Density (gm/ml)	Difference $(\rho-\rho_o)X10^{-6}$ (gm/ml)$X10^{-6}$
.000244	.998491	.998494	+3
.000757	.998633	.998630	-3
.001213	.998755	.998751	-4
.001857	.998919	.998922	+3
.002536	.999102	.999102	0

$$\rho = .26515\ C_2 + .99843$$

$$\bar{V} = .73598 \pm .00298 \text{ ml/gm}$$

FIGURE 15: A plot of the values in Table V. Density is plotted as a function of BSA concentration.

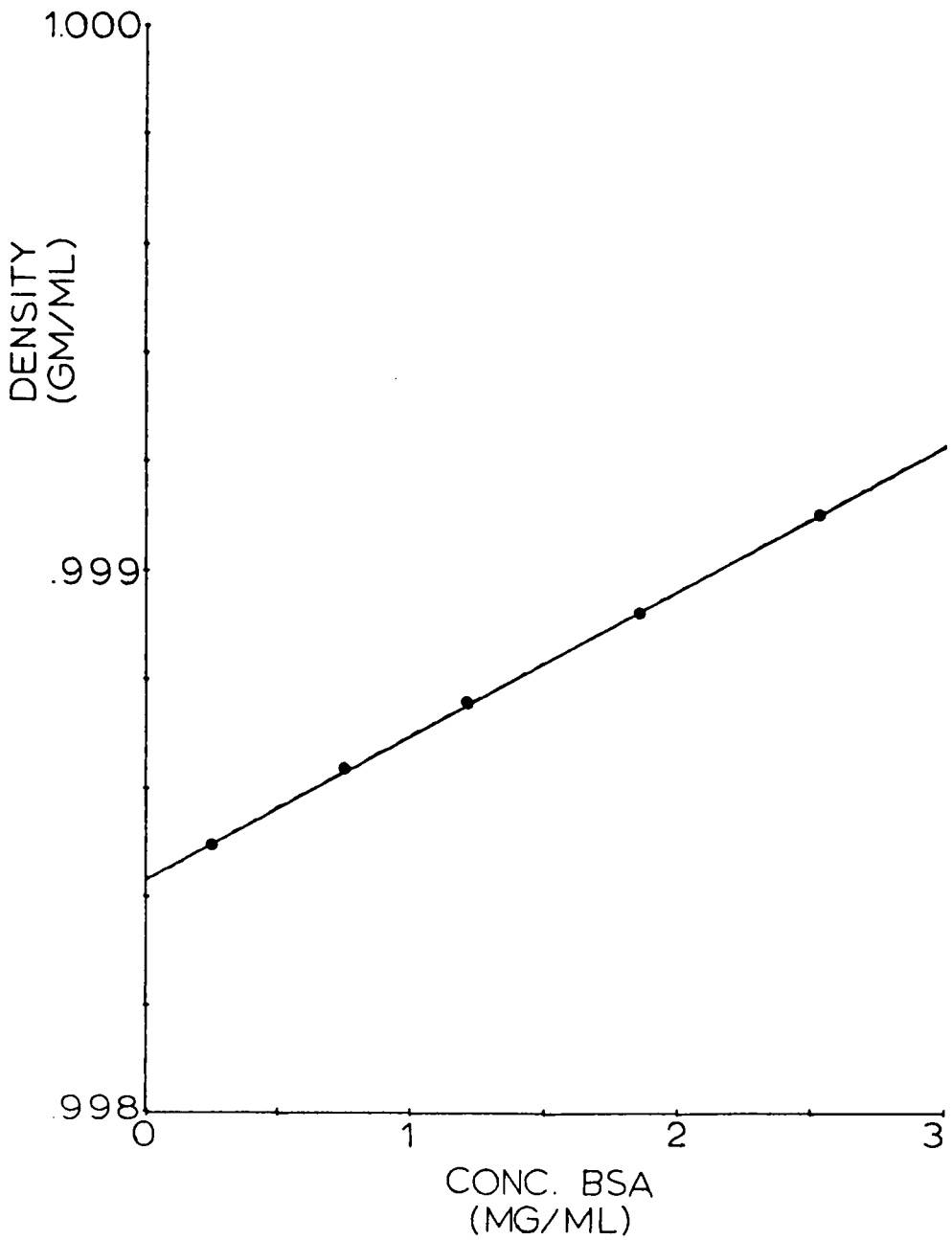
1.000
.999
.998
DENSITY
(GM/ML)
0
1
2
3
CONC. BSA
(MG/ML)

TABLE VI

$\overline{V}$ of Albumin in $CaCl_2$ Solution

Albumin Concentration (C_2) (gm/ml)	Density ρ_o (gm/ml)	Calculated Density (gm/ml)	Difference $(\rho - \rho_o) \times 10^{-6}$ (gm/ml) $\times 10^{-6}$
.000697	1.000248	1.000249	+1
.00121	1.000395	1.000386	-9
.00247	1.000718	1.000719	+1
.00352	1.000983	1.000994	+11
.00462	1.001281	1.001287	+6
.00569	1.001578	1.001568	-10

$$\rho = .26423\ C_2 + 1.00007$$

$$\overline{V} = .73577 \pm .00124 \text{ ml/gm}$$

FIGURE 16: A plot of the values in Table VI. Density is plotted as a function of BSA concentration.

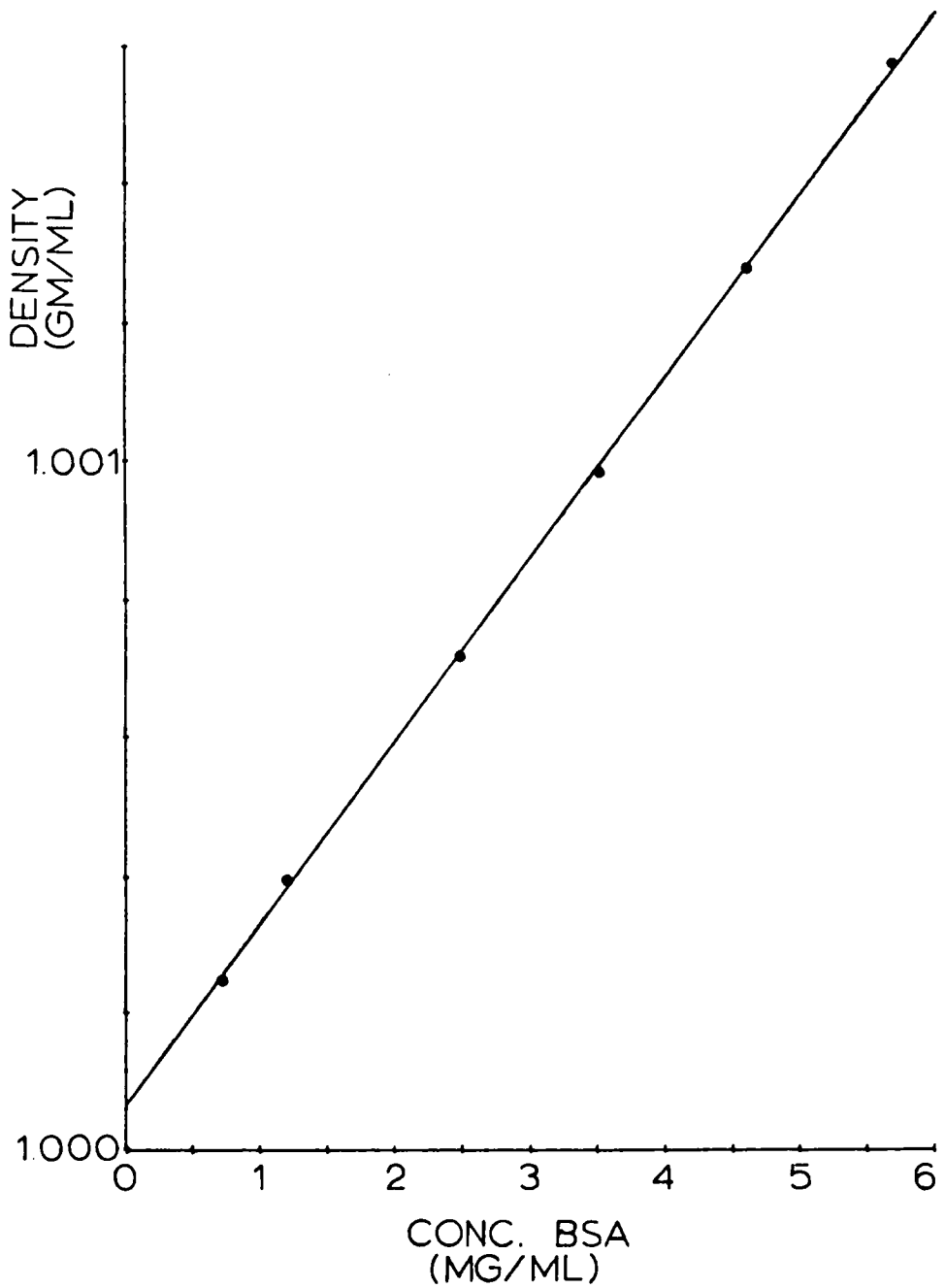
DENSITY
(GM/ML)
1.001
1.000
0
1
2
3
4
5
6
CONC. BSA
(MG/ML)

TABLE VII

$\bar{V}$ of Albumin in KCl Solution

Albumin Concentration (C_2) (gm/ml)	Density ρ_o (gm/ml)	Calculated Density (gm/ml)	Difference $(\rho-\rho_o)X10^{-6}$ $(gm/ml)X10^{-6}$
.00099	.999958	.999962	+4
.00217	1.000284	1.000281	-3
.00430	1.000861	1.000854	-7
.00535	1.001132	1.001138	+6

$$\rho = .26946\ C_2 + .99970$$

$$\bar{V} = .73076 \pm .00157 \text{ ml/gm}$$

FIGURE 17: A plot of the values in Table VII. Density is plotted as a function of BSA concentration.

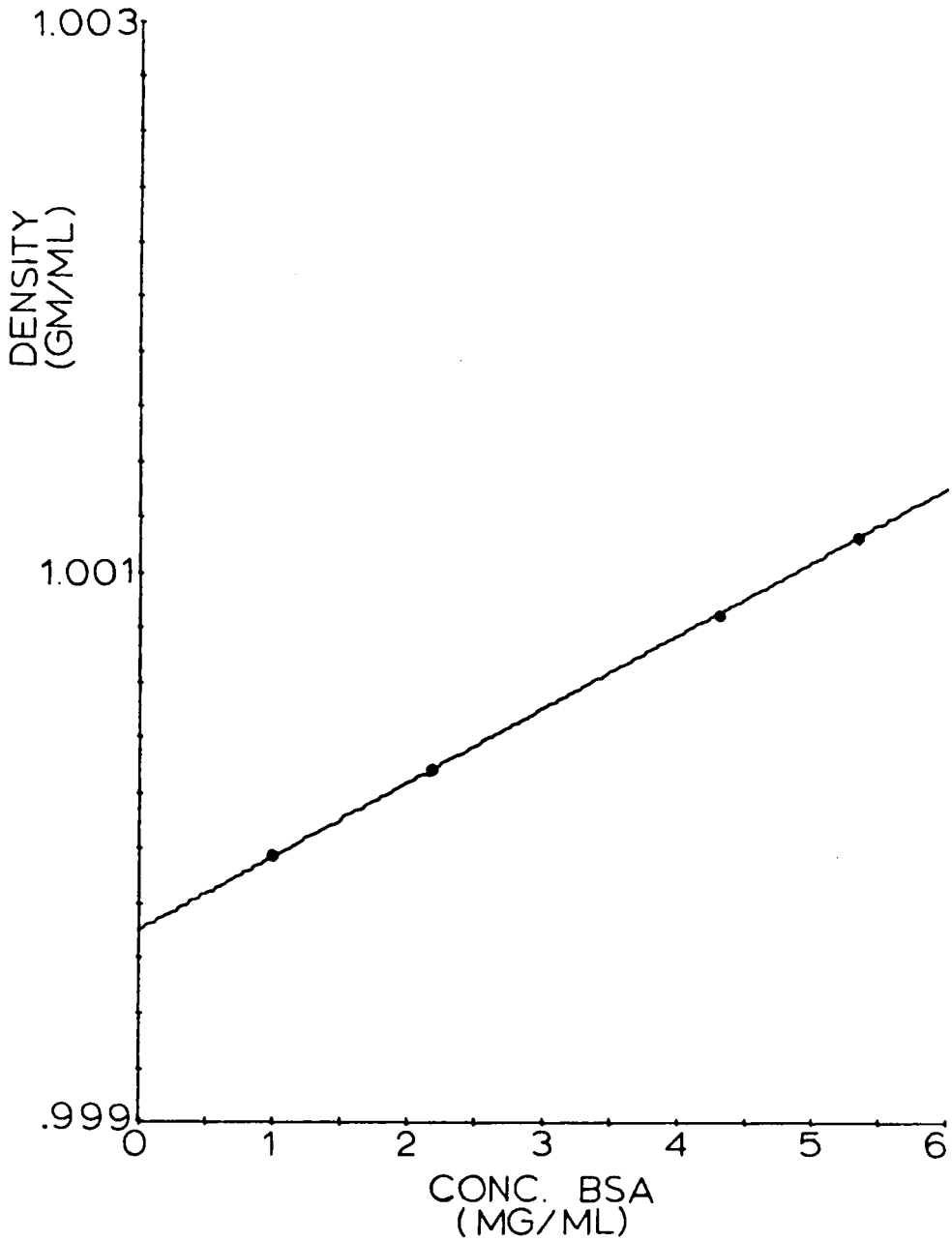
1.003
1.001
.999
DENSITY
(GM/ML)
0
1
2
3
4
5
6
CONC. BSA
(MG/ML)

$E^{280}_{1\,cm} = 6.14\ (\text{percent})^{-1}$. By reading the optical density and dividing by 6.14, the BSA concentrations were determined in units of percent or (mg/ml) X 10. Shown in Tables V, VI, and VII are the $\bar{V}$ measurements of BSA in distilled water, $CaCl_2$ solvent and KCl solvent respectively with the r.f. sensing densimeter. The values in these tables are plotted in Figures 15, 16, and 17 respectively. These are $\bar{V}_{[BSA]} = .736 \pm .003$ ml/mg in water, $\bar{V}_{[BSA]} = .736 \pm .001$ ml/mg in $CaCl_2$, $\bar{V}_{[BSA]} = .731 \pm .002$ ml/mg in KCl. There appears to be no difference in $\bar{V}_{[BSA]}$ in water and $\bar{V}_{[BSA]}$ in $CaCl_2$ solution. Upon performing an atomic absorption analysis with a Perkin Elmer Model 303 atomic absorption spectrophotometer, all samples were found contaminated with Ca, Mg, and a trace of Na. (See Table X.) Thus the indistinguishability of $\bar{V}_{[BSA]}$ in water and $CaCl_2$ buffer are to be expected. However, it can be seen that the $\bar{V}$ of BSA in $CaCl_2$ and KCl solvents can be distinguished. This difference in $\bar{V}$'s possibly reflects a conformational difference. Similar results have been obtained with poly-γ-benzyl-L-glutamate using dichloracetic acid as a denaturant in dichloroethylene solvent.[11,12] The mechanisms for such changes in protein conformation may be one or a combination of the following: (1) electrostatic repulsion between charges of a bound ionic ligand (Coulom repulsion);[13] (2) penetration of hydrophobic amino acid tails

into apolar regions of the macromolecules, resulting in replacement of conformation stabilizing segment-segment interactions by ligand-segment interactions (disruption of hydrophobic interactions);[13] (3) ratios of binding sites and their association constants in the native form to those in the unfolded form may be such that unfolding is favorable (entropy).[13] Thus conformational changes are predicted in the presence of charged ligands, and these can be detected by $\overline{V}$ measurements with a magnetic densimeter.

The $\overline{V}_{[BSA]}$ of .736 ± .003 ml/mg in water is in good agreement with the value of .734 ml/mg obtained from the Handbook of Biochemistry and Molecular Biology.[14] Therefore this instrument is capable of giving reliable absolute $\overline{V}$ measurements using Equation 49.

D. Partial Specific Volume Measurements of Bovine Serum Albumin in Distilled Water and Sodium Phosphate Buffer (pH 5.68), Using the Optical Sensing Densimeter

Table VIII and Figure 18 show data used in determining $\overline{V}_{[BSA]}$ in water using the optical sensing densimeter. Here all water was stored in pyrex glass containers as opposed to nalgene containers used with experiments in Section C. To prepare solutions, BSA (Schwartz-Mann Lot #X1422) was dissolved in distilled water and added to a dialysis bag for dialysis against distilled water. The dialysate was changed six times at intervals of twelve hours, and each dialysate

TABLE VIII

$\bar{V}$ of BSA in Distilled Water

BSA Concentration (C_2) (gm/ml)	Density ρ_o (gm/ml)	Calculated Density ρ (gm/ml)	Difference $(\rho - \rho_o) \times 10^{-6}$ (gm/ml) $\times 10^{-6}$
.000236	.998260	.998261	+1
.000373	.998299	.998297	-2
.000715	.998385	.998386	+1
.002119	.998755	.998754	-1

$$\rho = .26236\ C_2 + .998200$$

$$\bar{V}_{H_2O} = .7390$$

FIGURE 18: A plot of the values in Table VIII. Density is plotted as a function of BSA concentration.

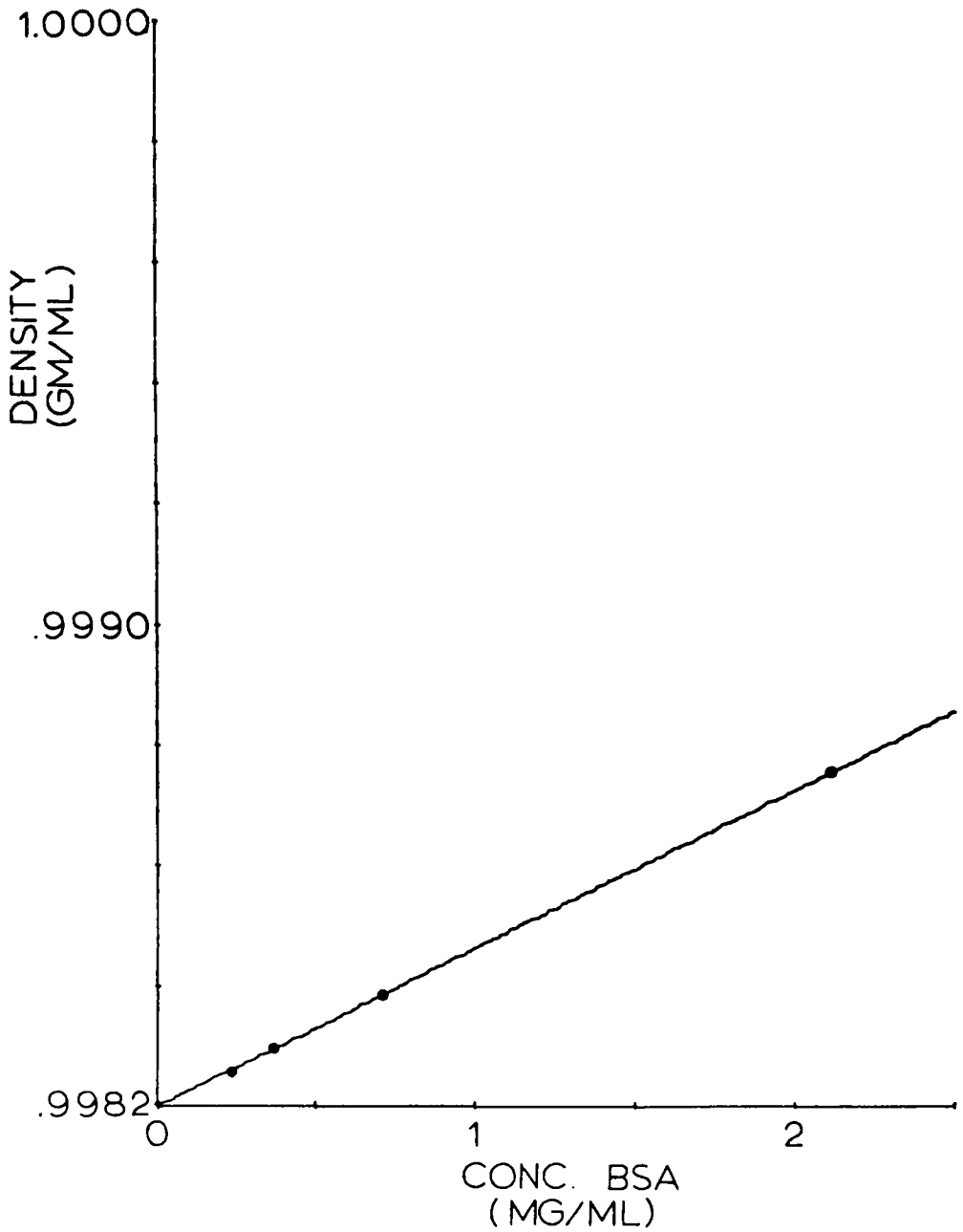
1.0000
.9990
.9982
DENSITY
(GM/ML)
0
1
2
CONC. BSA
(MG/ML)

change corresponded to a one-to-twenty dilution of dializable components. Three dilutions of the BSA solution with distilled water gave four BSA solutions, each with a different BSA concentration. BSA concentrations were determined spectrophotometrically using a $E^{280}_{1cm} = 6.14$ (percent)$^{-1}$. The $\overline{V}$ for this BSA in water is .739 ml/gm. This is in relative good agreement with the $\overline{V}_{[BSA]}$ determined above. The difference is probably due to the purer sample used here and lack of contaminants from nalgene containers. However, the relative error is still 0.68% from the value .734 ml/gm,[13] and 0.41% from the value obtained with the r. f. sensing densimeter.

Table IX and Figure 19 show data used in determining $\overline{V}_{[BSA]}$ in phosphate buffer. Here .01 M NaH_2PO_4 buffer was prepared and adjusted to pH 5.68 with concentrated NaOH without appreciably changing the solution volume. Crystalline BSA (Schwartz-Mann Lot #X1422) was added directly to the buffer and this solution was diluted with buffer to give several BSA solutions of different BSA concentration. Each BSA concentration was determined using a $E^{280}_{1cm} = 6.14$ (percent)$^{-1}$. The $\overline{V}$ of BSA here is .747 ml/gm.

E. Preferential Interactions

Recalling that for any reaction

$$\Delta G = \Delta E + P\Delta V - T\Delta S \qquad (52)$$

TABLE IX

$\overline{V}$ of BSA in Phosphate Buffer pH 5.68

BSA Concentration (C_2) (gm/ml)	Density ρ_o (gm/ml)	Calculated Density ρ (gm/ml)	Difference $(\rho-\rho_o)X10^{-6}$ (gm/ml)$X10^{-6}$
.0000	.999139	.999147	+8
.0009322	.999382	.999383	+1
.0019377	.999649	.999637	-12
.0029025	.999882	.999882	0
.011581	1.002078	1.002080	+2

$$\rho = .25323\ C_2 + .999147$$

$$\overline{V}_{PO_4} = .7474$$

FIGURE 19: A plot of the values in Table IX. Density is plotted as a function of BSA concentration.

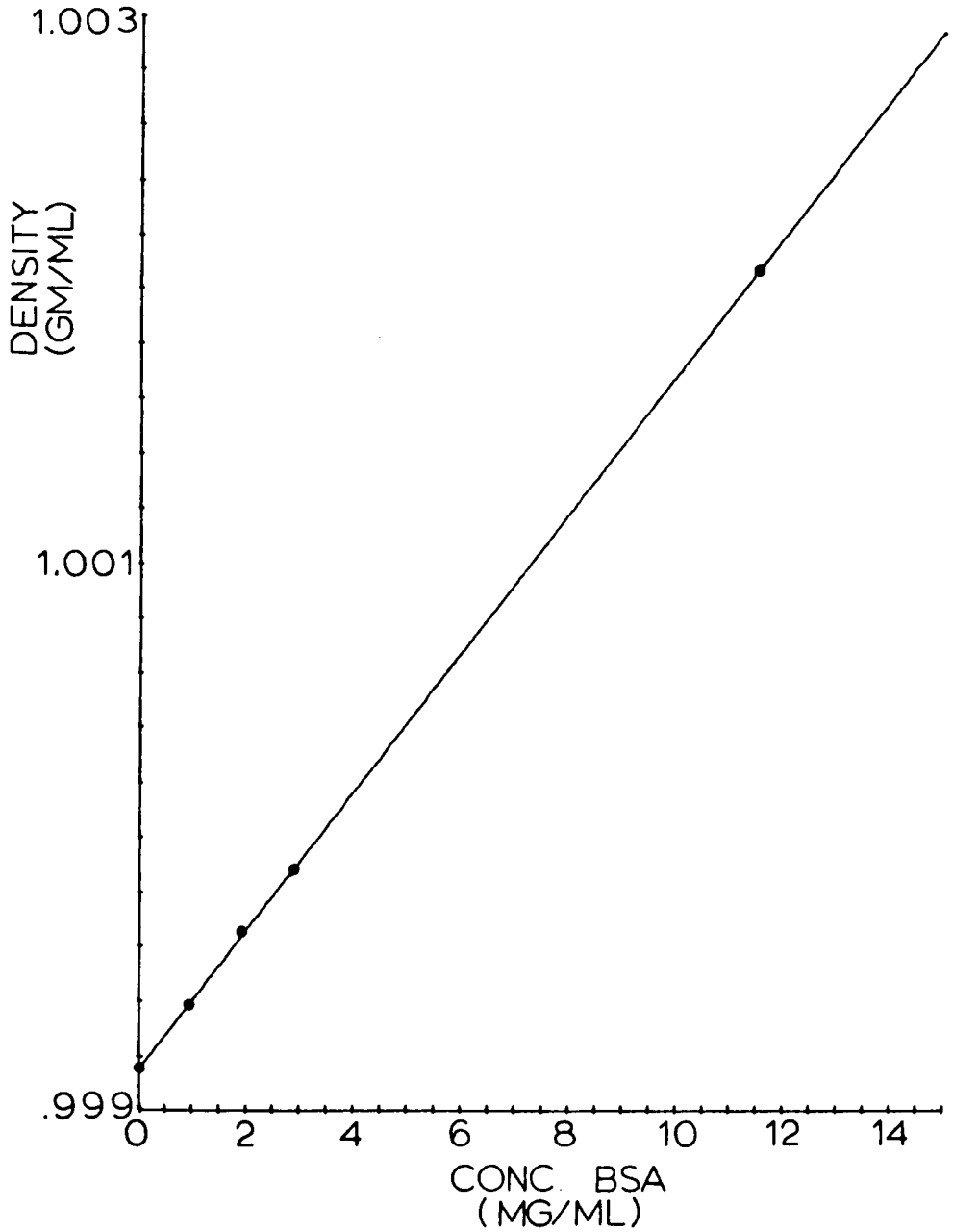
1.003
1.001
.999
DENSITY
(GM/ML)
0
2
4
6
8
10
12
14
CONC BSA
(MG/ML)

TABLE X

Atomic Absorption Data on BSA Samples

Solvent	[BSA] (%)	Concentration of Components [Ca] (µg/ml)	[Mg] (µg/ml)	[Na] (µg/ml)	[K] (µg/ml)
H_2O	.0244	135.0	92.5	0.10	--
	.0757	127.5	77.5	1.5	--
	.1213	162.5	95.0	1.4	--
	.1857	127.5	77.5	1.6	--
	.2536	162.5	92.5	1.5	--
$CaCl_2$	.0697	800.0	92.5	1.1	--
	.121	825.0	100.0	1.6	--
	.247	775.0	100.0	2.0	--
	.352	800.0	100.0	2.5	--
	.462	800.0	100.0	4.0	--
	.569	800.0	100.0	2.4	--
KCl	.099	57.5	77.5	--	821
	.217	57.5	75.0	--	820
	.430	57.5	72.5	.20	820
	.535	57.5	75.0	.40	820

at constant temperature (T) and pressure (P), most physical chemists measure the energy (E) and entropy (S) changes, neglecting the change in volume (ΔV) since ΔE is nearly equivalent to ΔH ($\Delta H = \Delta E + P\Delta V$). ($P\Delta V$ can be neglected since this term is almost always much smaller than ΔE.) However, if accurate measurements can be made of ΔV, it may be that this quantity does not reflect changes seen by these traditional reaction probes which measure only ΔE and ΔS. In ΔV one sees volume changes resulting from changes in partial volumes of each component when chemical bonds are broken and/or formed and/or where secondary structures are changed during a reaction. It is the latter events which are most important when proteins are involved.[4] As has been shown earlier measurable $\overline{V}$ changes without primary structure changes of proteins can and do occur. If (1) total masses are properly accounted for and (2) if partial volume measurements are feasible, the overall ΔV for a process can be separated into quantities related to each component by the following relation:

$$V = \sum_{i=1}^{N} m_i \overline{V}_i \qquad (53)$$

With the proper experimental protocol conditions, 1 and 2 can be satisfied.

The apparent specific volume ϕ is given by

$$\phi_i = \bar{V}_i - m_i \left(\frac{\partial \phi_i}{\partial m_i}\right)_{m_j, T, P \quad j \neq i} \tag{54}$$

and is the most convenient parameter to measure. At vanishing m_i, ϕ_i becomes equal to V_i. In a multi-component system with components 1, 2, 3,...,i,...N the partial specific volumes of each component prior to and after reaction can be determined. To determine $\bar{V}_i$ of the ith component prior to reaction, the solution density as a function of C_i only <u>in the inert solvent</u> is measured and $\bar{V}_i$ is obtained from Equation 51.

$$\rho = f(C_i) \tag{55}$$

To determine $\bar{V}_i$ after reaction ρ is measured as a function of each component.

$$\rho = f(C_1, C_2, \ldots, C_i, \ldots C_N) \tag{56}$$

Again $\bar{V}_i$ is determined by Equation 51, except $\left(\frac{\partial \rho}{\partial C_i}\right)$ is not measured at $m_j = 0$ $(j \neq i)$ and ρ_o becomes the solution density without component i present.

This concept is most easily illustrated by a three-component system, where the first component is an inert solvent, the second component is a protein and the third component is a ligand that binds to the protein at

FIGURE 20: A three dimensional plot of the theoretical results of a titration experiment. It is assumed there is only one set of binding sites, each with the same equilibrium constant.

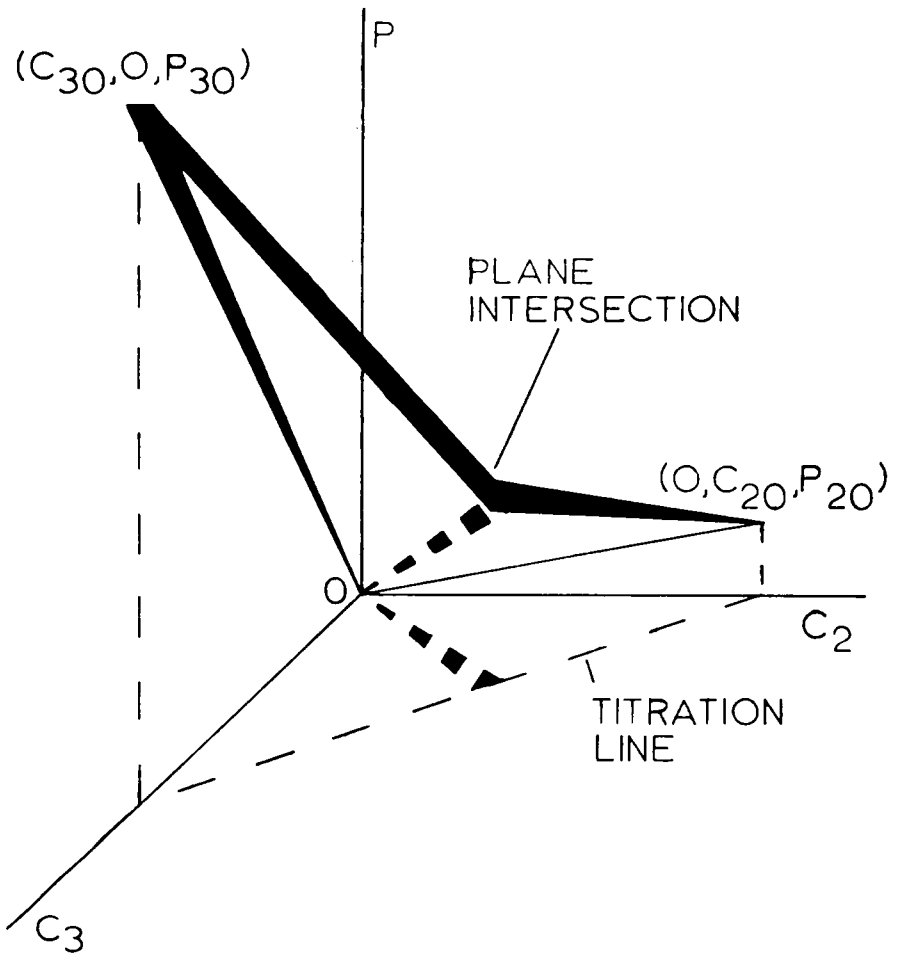
P
(C_{30},O,P_{30})
PLANE
INTERSECTION
(O,C_{20},P_{20})
O
C_2
TITRATION
LINE
C_3

FIGURE 21: A view of Figure 20 looking down the ρ axis showing C_2 as a function of C_3 durring a titration, and showing the directional derivatives corresponding to the two values of $\bar{V}_2$. $(\partial\rho/\partial C_2)_a$ corresponds to $\bar{V}_{2i}$ and $(\partial\rho/\partial C_2)_b$ corresponds to $\bar{V}_{2f}$.

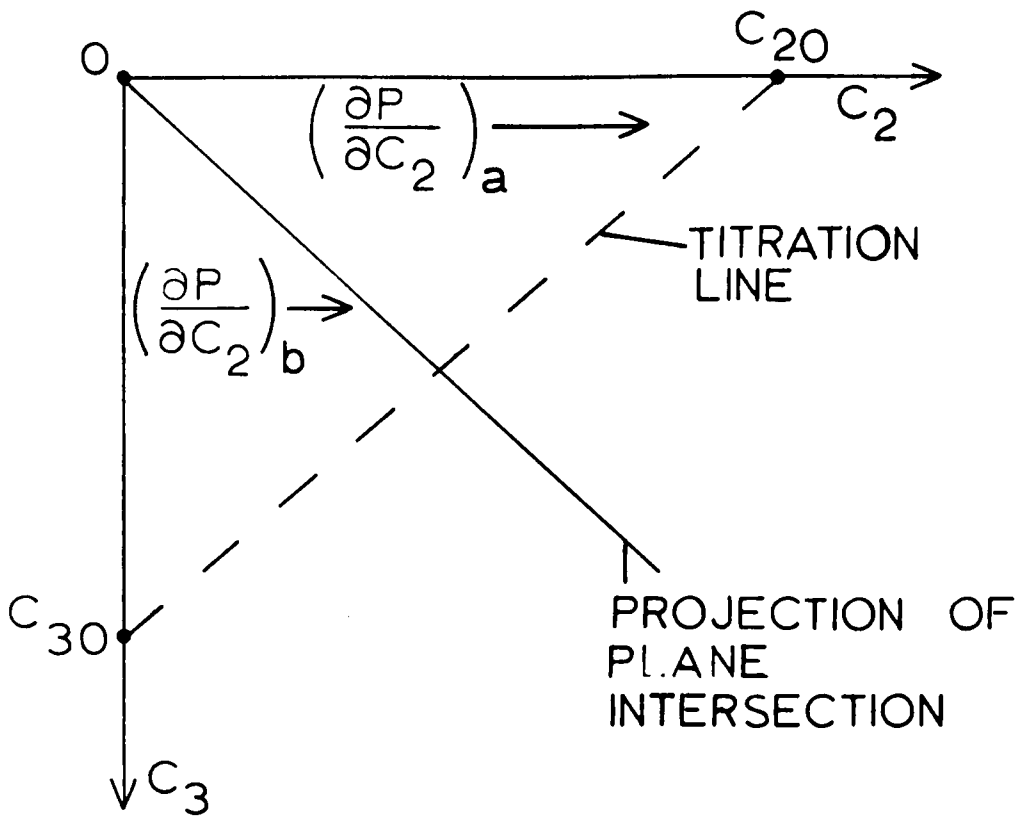
0
C_{20}
C_2
$\left(\frac{\partial P}{\partial C_2}\right)_a$
TITRATION LINE
$\left(\frac{\partial P}{\partial C_2}\right)_b$
C_{30}
PROJECTION OF PLANE INTERSECTION
C_3

only one type of site. Using a three-dimensional plot with orthogonal coordinates C_3, C_2 and ρ, this system can be geometrically represented. The experimental procedure calls for measuring ρ as a function of C_3 only to determine $\overline{V}_{3_i}$ ($\overline{V}_3$ prior to reaction) and ρ as a function of C_2 only to determine $\overline{V}_{2i}$ ($\overline{V}_2$ prior to reaction). To determine $\overline{V}_{3f}$ and $\overline{V}_{2f}$ ($\overline{V}$'s after mixing) a buffer solution containing only component 2 is "titrated" with a buffer solution containing only component 3. Mechanically this is carried out by adding a known mass of solution containing component 2 and recording its density with a magnetic densimeter. Next, a known mass of solution containing component 3 is added, and the density of this mexture is recorded. Further mass increments of solution containing component 3 are added and the solution density recorded after each addition. Hypothetical results of such an experiment are shown in Figure 20. Two different planes are found to intersect at a line passing through the origin. The path followed through the C_3, C_2 plane is a straight line from the point $(0, C_{20})$ to the point $(C_{30}, 0)$. If $\Delta V = 0$ for the reaction of components 3 and 2, the line followed from $(0,C_{20},\rho_{20})$ to $(C_{30},0,\rho_{30})$ is a straight line. However, if ΔV is nonzero, the path followed is not a straight line but the path indicated by the solid line in Figure 20 (if $\Delta V > 0$). Figure 21 is used to illustrate the abstraction of the $\overline{V}$'s.

$\left(\frac{\partial \rho}{\partial C_2}\right)_a$ is used in Equation 51 to obtain $\bar{V}_{2i}$ and $\left(\frac{\partial \rho}{\partial C_2}\right)_b$ is used in Equation 51 to determine $\bar{V}_{2f}$ after reaction with component 3. Likewise $\left(\frac{\partial \rho}{\partial C_3}\right)$ in each region is different and $\bar{V}_{3i}$ and $\bar{V}_{3f}$ can be determined. Thus one can experimentally determine the $\bar{V}$ of each component prior to and after reaction.

To check the feasibility of such determinations using a magnetic densimeter $CaCl_2$ and $FeCl_3$ were used as ligands and Bovine Serum Albumin was used as the protein. In this experiment BSA (Sigma Fraction V, Lot #A-4503) was dialyzed against distilled water in dialysis tubing, with the dialysate being changed six times at eight-hour intervals. Each change corresponded to a 1:20 dilution of dializable components. The A_{280} of the BSA solution indicated a protein concentration of .103%. This solution was titrated with a $CaCl_2$ solution and a $FeCl_3$ solution whose concentrations were determined by atomic absorption. The atomic absorption data are shown in Table XII. In this experiment, since the only purpose of the experiment was to determine if an intersection of two planes could be detected, the float used was not calibrated with standard sucrose solutions. Hence only densimeter reading as a function of the ratio of salt solution volume to total solution volume (V_S/V_T) added was recorded in Table XI and plotted in Figures 22 and 23. As can be seen in these figures, the

TABLE XI

Titration of BSA with $CaCl_2$ and $FeCl_3$: Detection of Change of $\bar{V}$'s

Salt Solution	$\frac{\text{Salt Solution}}{\text{Total Solution}}$ ($\frac{V}{\%\bar{V}_T}$)	Densimeter Reading (Volts)
$CaCl_2$	0	.16455
	.335	.16475
	.667	.16499
	.997	.16522
	2.29	.16645
	2.93	.16705
	3.56	.16767
$CaCl_2$	0	.16484
	.335	.16510
	.667	.16540
	.997	.16572
	2.29	.16735
	2.93	.16812
	3.56	.16892
$FeCl_3$	0	.16469
	.167	.16495
	.335	.16520
	.502	.16545
	.667	.16600
	.832	.16655
	.997	.16710
	1.162	.16765
$FeCl_3$	0	.16475
	.167	.16500
	.335	.16525
	.502	.16550
	.667	.16605
	.832	.16660

FIGURE 22: A plot of the falues for $CaCl_2$ in Table XI. Densimeter reading is plotted as a function of the volume fraction of $CaCl_2$ solution present.

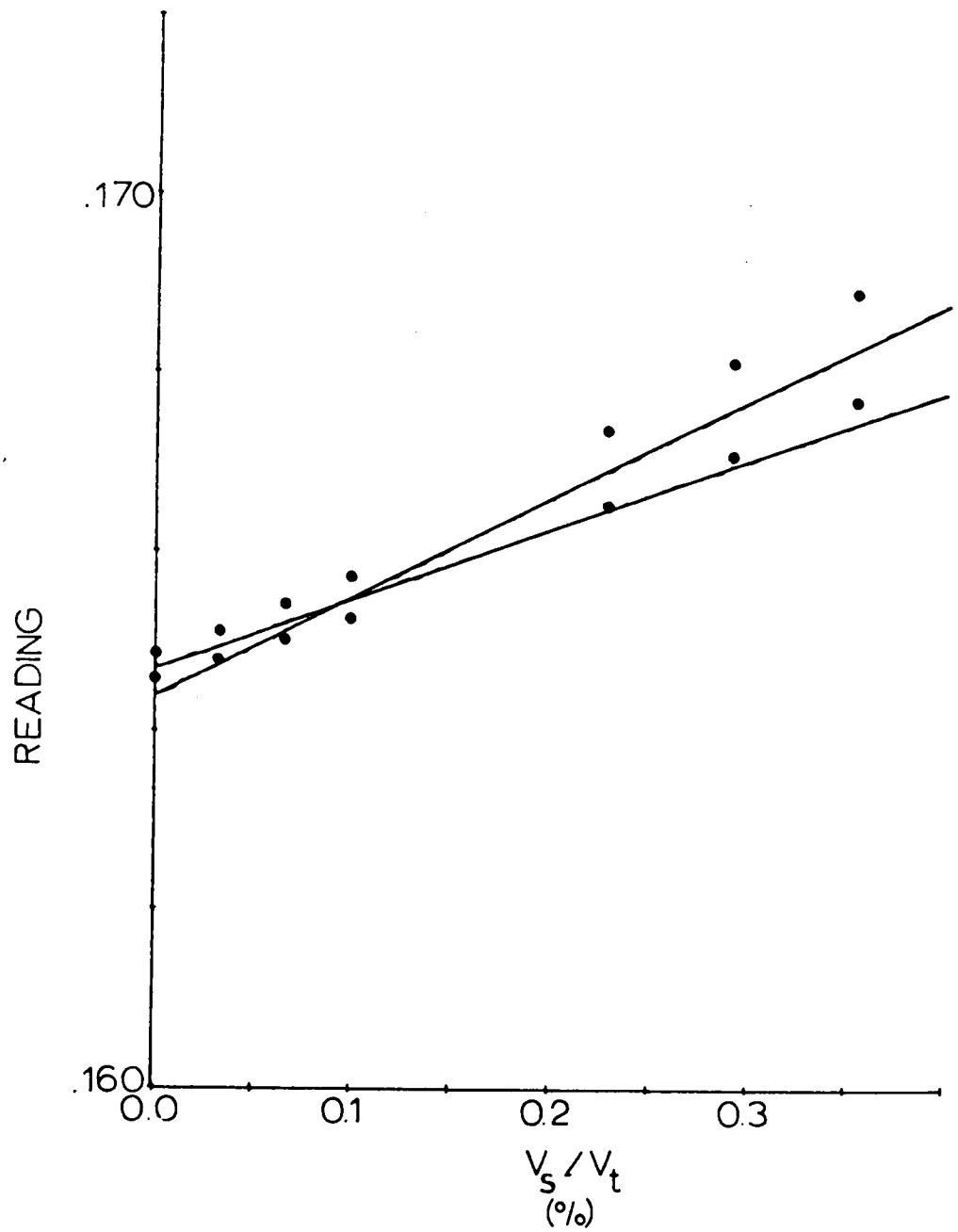
.170
.160
READING
0.0
0.1
0.2
0.3
V_s / V_t
(%)

FIGURE 23: A plot of the values for $FeCl_3$ in Table XI. Densimeter reading is plotted as a function of the volume fraction of $FeCl_3$ solution present.

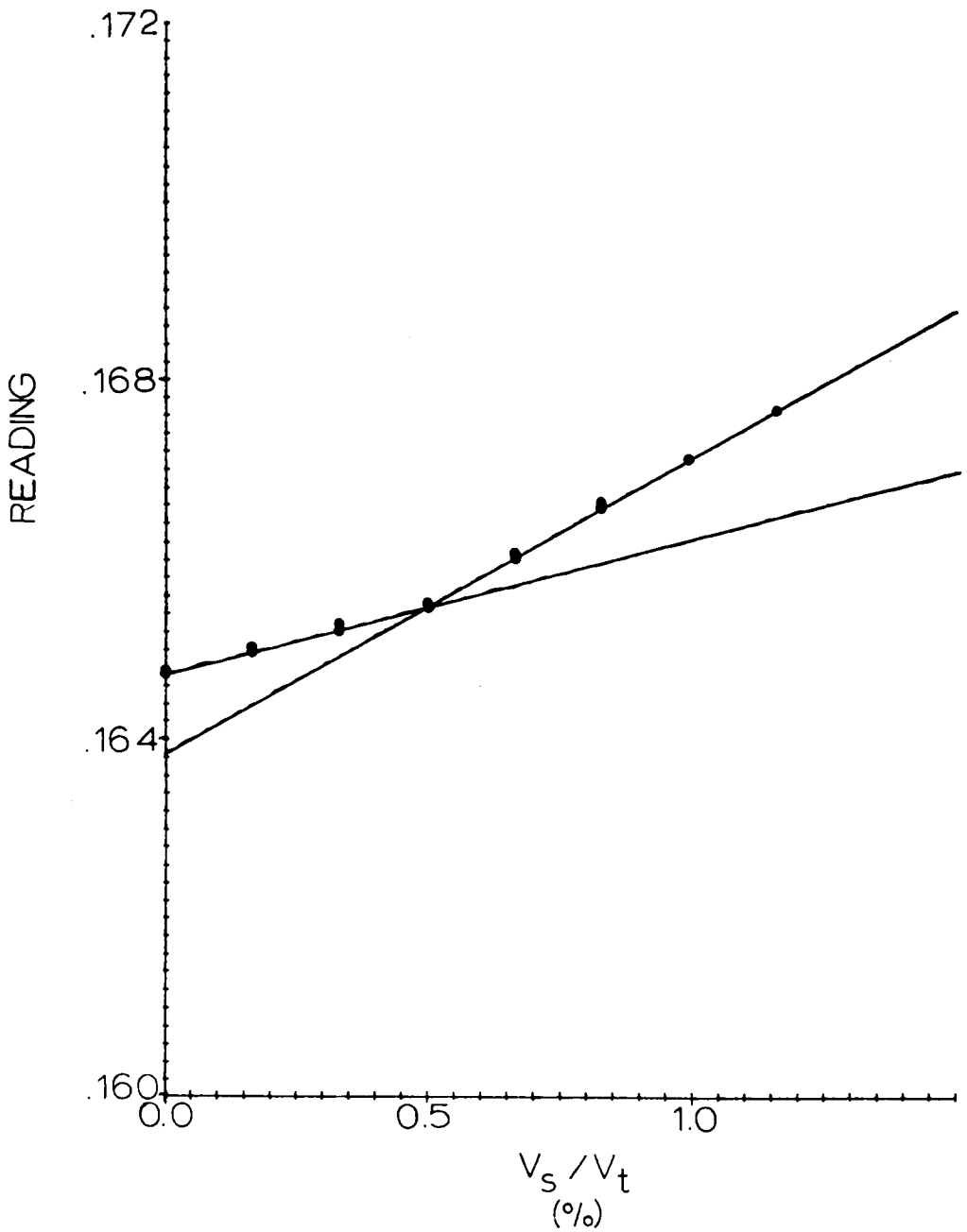
.172
.168
.164
.160
READING
0.0
0.5
1.0
V_s / V_t
(%)

TABLE XII

Atomic Absorption Data on Solutions in Table XI

	Concentrations ($\frac{\mu g}{ml}$)			
Solution	[Ca]	[Na]	[K]	[Fe]
$CaCl_2$	1937.5	Tr	Tr	0.0
$FeCl_3$	137.5	.60	Tr	5000.0
Al	.7	.5	Tr	Tr
Dist. H_2O	.0006	.0115	--	.004

magnetic densimeter is sensitive enough to detect the volume changes accompanying a change in the $\bar{V}$ of the BSA upon addition of $CaCl_2$ and $FeCl_3$. The values of V_S/V_T where the transitions occur have no meaning in terms of binding site numbers or equilibrium constants because the amounts of free ligand in solution cannot be determined. Thus the only quantities that can be determined in an experiment of this type at this time are as follows: (1) the overall ΔV of reaction and (2) the $\Delta\bar{V}$'s of the individual component.

To determine the actual overall ΔV of a reaction, another experiment was performed. Here BSA (Schwartz-Mann Lot #X1422) from the bottle was added to .01 M phosphate buffer at pH 5.68. Methyl orange (MO) (Coleman and Bell Lot #440914) was dissolved in the same buffer. The BSA concentrations were determined using an $E^{280}_{1\,cm} = 6.14$ (percent)$^{-1}$ and the MO concentrations were determined using an $E^{280}_{1\,cm} = 2.69 \times 10\ M^{-1}$.[15] Three dilutions of the original dye solution were made to get into its linear absorbance region. The concentration of BSA in the protein only solution was 2.9025 mg/ml and the MO concentration in the ligand only solution was .7864 mg/ml. Table XIII shows density as a function of both MO and BSA concentration when the BSA solution is titrated with the MO solution in two different experiments. Table XIV shows density as a function of MO and BSA concentration when the MO solution is

titrated with the BSA solution. Tables XIII and XIV also show the $\Delta V/V$ of reaction as a function of MO and BSA concentration. A plot of density as a function of MO concentration is shown in Figure 24. A plot of $\Delta V/V$ as a function of MO concentration is shown in Figure 25. Unfortunately there are no data available on the ΔV of reaction between BSA and MO. However, $\frac{\Delta V}{V}$ appears to be a linear function of total methyl orange concentration to an accuracy of better than $\pm 5 \times 10^{-7}$ giving a ΔV accuracy to about $\pm 7.5 \times 10^{-7}$ ml, as determined by the relation

$$\Delta V = \left(\frac{m_1 + m_2}{\rho}\right) \quad \left(\frac{m_1}{\rho_1} + \frac{m_2}{\rho_2}\right) \tag{57}$$

where ρ is the density of the solution containing m_1 grams of solution 1, and m_2 grams of solution 2, and ρ_1 and ρ_2 are solution densities of solutions 1 and 2 respectively.

The two linear fits to the data in Table XI (Figures 22 and 23) and the linear fits in Tables XIII and XIV (Figure 24) of density as a function of ligand concentration show that the intersection of two planes in Figure 20 is a reasonable representation of experimental results within the range of experimental error. This also shows that Equation 54 is valid and that at vanishing m_i, $\emptyset = \overline{V}_i = \frac{1}{\rho_o}\left(1 - \left(\frac{\partial \rho}{\partial C_i}\right)\right)$.

TABLE XIII

Titration of BSA with Methyl Orange in .01M Phosphate Buffer, pH 5.68

Concentration		Measured Density	Calculated Density				
[MO] gm/ml	[BSA] gm/ml	ρ_{meas} gm/ml	ρ_{calc} gm/ml	$\Delta\rho \times 10^{-6}$ gm/ml	$-\frac{\Delta V}{V}_{meas}$	$-\frac{\Delta V}{V}_{calc}$	$\Delta(\frac{\Delta V}{V})$ $\times 10^{-7}$
.0000	.0029025	.999882	.999882	0	0	.00000044	+4.4
.0000107	.0028629	.999871	.999877	+6	.0000012	.00000093	-2.7
.0000222	.0028206	.999871	.999871	0	.0000018	.00000145	-3.5
.0000530	.0027067	.999862	.999854	-8	.0000027	.00000284	+1.4
.0001276	.0024317	.999815	.999814	-1	.0000059	.00000621	+3.1
.0002219	.0020835	.999759	.999764	+5	.0000107	.00001047	-2.3
.0002149	.0021093	.999768	.999768	0	.0000106	.00001015	-4.5
.0002863	.0018460	.999731	.999729	-2	.0000130	.00001338	+3.8

$$[BSA] = -3.69027753[MO] + .00290243924 \qquad r = .99999996$$

$$\rho = -.53535139[MO] + .99988255 \qquad r = .99794036$$

$$\frac{\Delta V}{V} = .04516691[MO] + .00000044 \qquad r = .99746714$$

TABLE XIV

Titration of Methyl Orange with BSA in .01M Phosphate Buffer, pH 5.68

Concentration		Measured Density	Calculated Density				
[MO] gm/ml	[BSA] gm/ml	ρ_{meas} gm/ml	ρ_{calc} gm/ml	$\Delta\rho X10^{-6}$ gm/ml	$-\frac{\Delta V}{V}_{meas}$	$-\frac{\Delta V}{V}_{calc}$	$\Delta(\frac{\Delta V}{V})$ $X10^{-7}$
.0007864	.000	.999426	.999429	+3	.000000	.0000061	+61
.0007686	.0000643	.999448	.999442	-6	.0000141	.0000080	-61
.0006665	.0004425	.999512	.999514	+2	.0000185	.0000187	+2
.0005868	.0007410	.999562	.999570	+8	.0000277	.0000271	-6
.0005700	.0007987	.999585	.999582	-3	.0000306	.0000288	-18
.0005218	.0009765	.999620	.999611	-9	.0000316	.0000339	+23

$$[BSA] = -3.69386463[MO] + .00290433466$$

$$\rho = -.70457[MO] + .99998337$$

$$\frac{\Delta V}{V} = -.10496927[MO] + .00008864$$

FIGURE 24: A plot of density as a function of methyl orange concentration from Tables XIII and XIV.

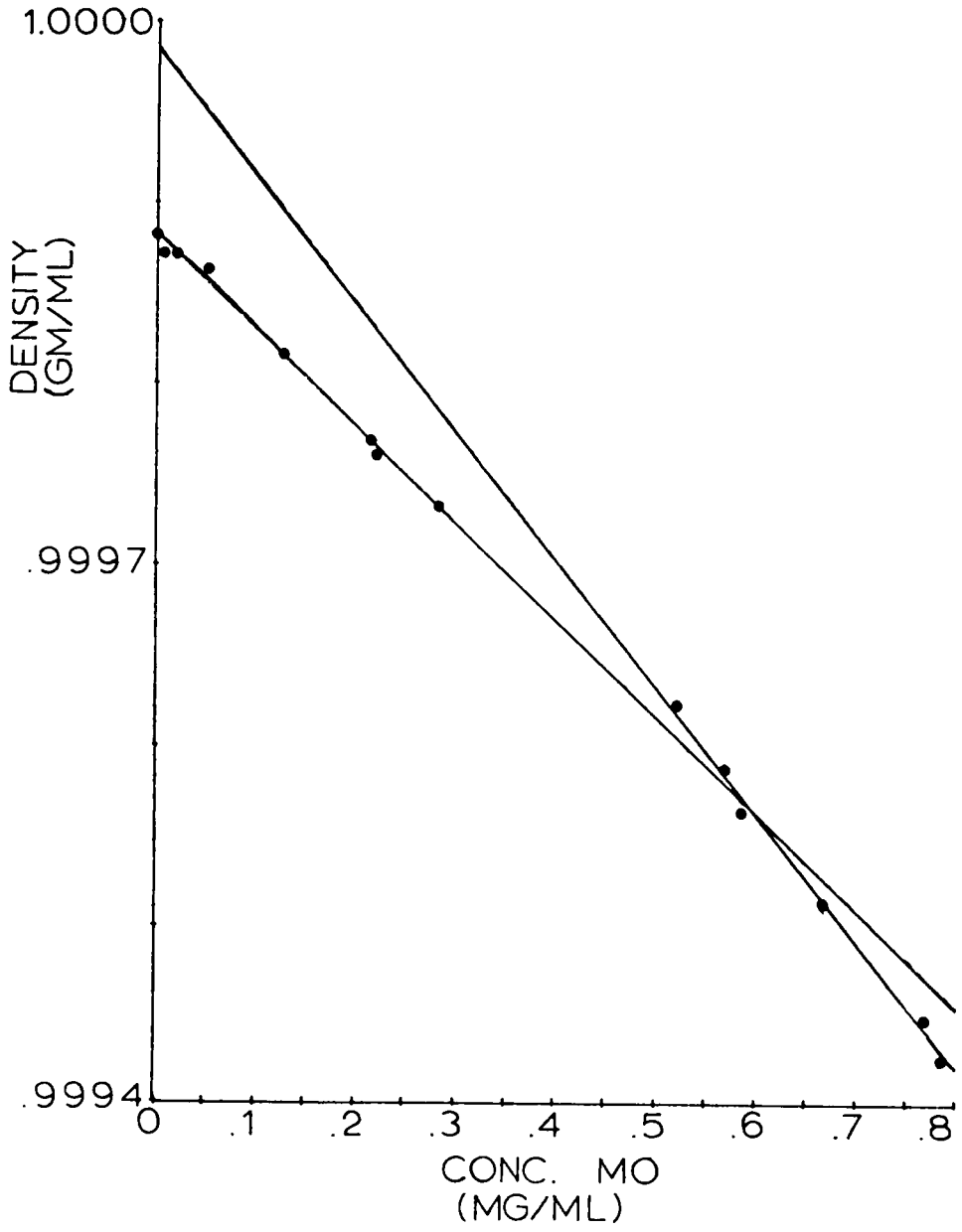
1.0000
.9997
.9994
DENSITY
(GM/ML)
0
.1
.2
.3
.4
.5
.6
.7
.8
CONC. MO
(MG/ML)

FIGURE 25: A plot of $\Delta V/V$ as a function of methyl orange concentration from Tables XIII and XIV.

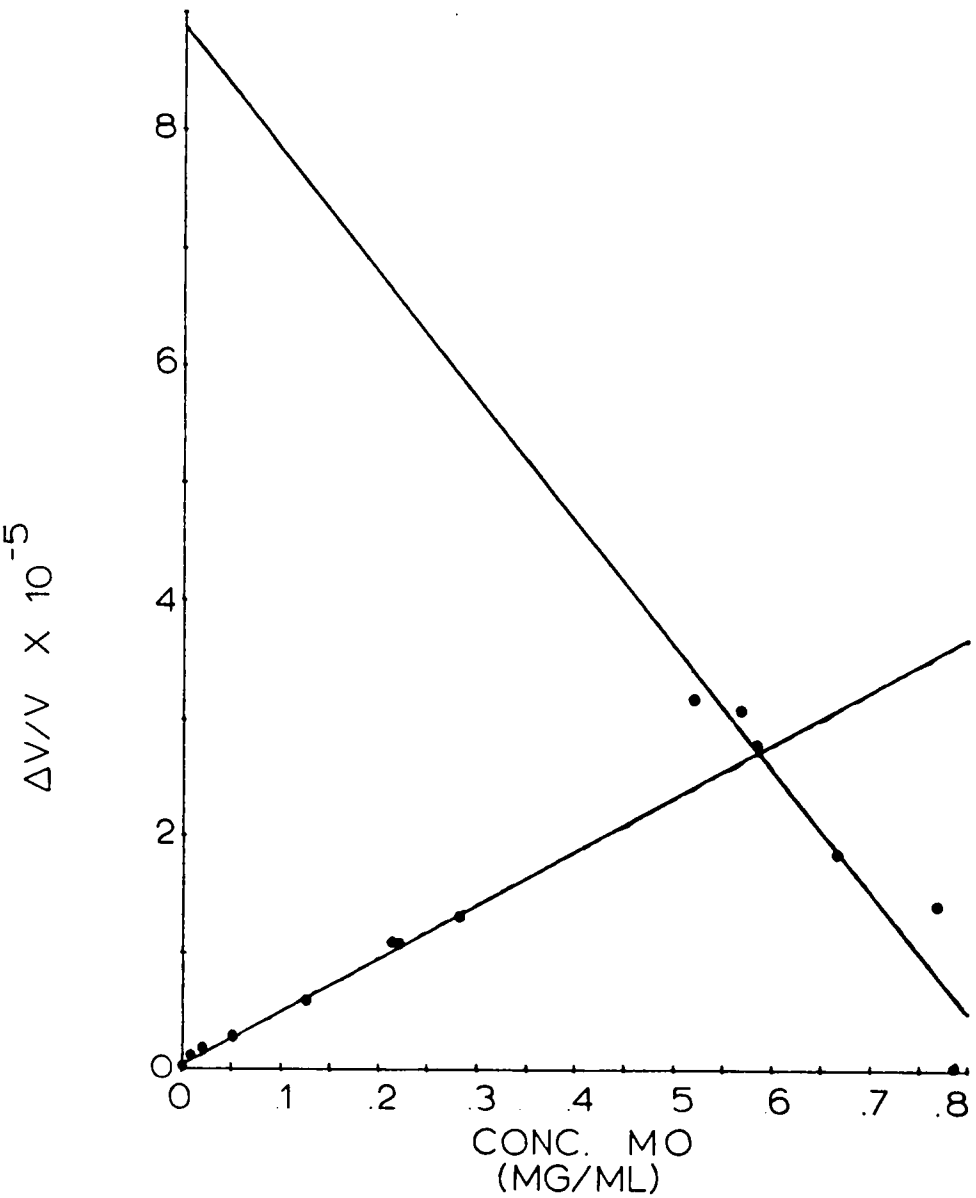
ΔV/V X 10^-5
8
6
4
2
0
0
.1
.2
.3
.4
.5
.6
.7
.8
CONC. MO
(MG/ML)

V. CONCLUSION

Both r. f. and optical sensing densimeters have been built and tested. These instruments have been shown capable of measuring densities accurately to within ± 12 μg/ml with a precision of ± 5 μg/ml. They are, therefore, both capable of determining partial specific volumes. The key to this ability is the repositioning of the float in the magnetic field and maintaining this position constant. Although in the first experiments there was little problem with the r.f. sensing densimeter in this respect, the 60 cycle radiation emitted by the Haake Model FS-0-1000 temperature controller interfered drastically with the sensing system. The net effect was the introduction of 60 cycle modulation into the oscillator circuit which was translated to float motion. This effect could easily be seen with an oscilloscope at all stages preceding the control amplifier; in fact, a .1 volt peak to peak 60 cycle voltage could be detected between any two points on the chasis, even though the chasis was grounded. Several attempts were made to remedy this problem, including changing power supplies, changing the r.f. amplifier circuit and filters, but none of these were completely successful. Hence the optical sensing system was developed.

The optical sensing system uses a light source of constant intensity and a light sensing diode. The advantage

here is that in the light source any 60 cycle noise is "averaged" out since the incandescent filament does not respond instantly to small rapid fluctuations in current. Thus with room lighting completely shut out of the temperature bath and sample cell, problems with 60 cycle noise and random voltage spikes are eliminated in this system, with the only apparent problem being the use of turbid solutions. The control system which was the same for both systems worked well in each case.

Relatively little problem was encountered in making $\bar{V}$ measurements with these instruments other than those already mentioned. The $\bar{V}_{[BSA]}$ determined by each instrument is in relatively good agreement with the accepted value. Thus these instruments are capable of measuring partial specific volumes to within ±.004 ml/gm provided there are no interface problems between the float and solution (as is the case with lipid systems). Based on measurements of $\bar{V}$'s of BSA in various solvents it has been shown that the partial specific volume of a protein is a function of solvent, which is due to the interaction of individual solvent molecules with the protein molecules on the molecular level. Hence by using Equation 51, $\bar{V}$'s of a protein can be determined and distinguished by these instruments. Furthermore, a convenient way of distinguishing $\bar{V}$'s as a function of

solvent compositon appears to be by "titration" experiments similar to the one described in Section IIIE with methyl orange and bovine serum albumin.

APPENDIX A

Temperature Control

For water

$$\rho_{21°C} = 0.997992 \tag{58}$$

$$\rho_{19°C} = 0.998405 \tag{59}$$

hence

$$-(\Delta\rho/\Delta T)_w = 2.065 \times 10^{-4} \text{ gm/(ml - °C)}. \tag{60}$$

The linear co-efficient of expansion for pyrex is 3.25×10^{-6}. The bulk co-efficient of expansion being three times the linear co-efficient is $\beta = .0975 \times 10^{-4}$ $(°C)^{-1}$.

$$(\rho_B \beta_B) = -(\Delta\rho/\Delta T)_B \tag{61}$$

$$\rho_B \simeq .99 \tag{62}$$

Thus

$$-(\Delta\rho/\Delta T)_B = .0965 \times 10^{-4} \text{ gm/(ml - °C)} \tag{63}$$

$$(\Delta\rho_w - \Delta\rho_B) = \Delta T(\rho_w\beta_w - \rho_B\beta_B) \tag{64}$$

$$\Delta T = \frac{(\Delta\rho_w - \Delta\rho_B)}{\rho_w\beta_w - \rho_B\beta_B} \tag{65}$$

setting

$$(\Delta\rho_w - \Delta\rho_B) = 10^{-6} \text{ gm/ml} \tag{66}$$

$$\Delta T = \frac{10^{-6}}{(2.065 - .097) \times 10^{-4}} = .0051°C \tag{67}$$

Thus temperature changes of .0051°C are sufficient to cause density changes of 1 μg/ml.

APPENDIX B

Pressure Effects

The compressibility (K) of water at 20°C is 4.58×10^{11} $cm^2/dyne$

$$K = \frac{1}{V} \frac{\Delta V}{\Delta P} \tag{68}$$

$$K = \frac{1}{\rho} \frac{\Delta \rho}{\Delta P} \tag{69}$$

$$\Delta P = \frac{\Delta \rho}{K \rho} \tag{70}$$

setting ρ equal to .998387 and $\Delta\rho$ equal to 10^{-6} gm/ml

$$\Delta P = .219 \times 10^5 \text{ dynes/cm}^2 = .0216 \text{ atm.} \tag{71}$$

Over a period of several days pressure changes of several times this magnitude may occur. However, absolute density is not as important as density changes detected over a range of solutions and these measurements can be made in one day in which atmospheric pressure changes are usually less than .02 atm.

APPENDIX C

Determination of the Extinction Coefficient of Bovine Serum Albumin

Because the extinction coefficient of $E^{280}_{1cm} = 6.6$ $(percent)^{-1}$ gave $\bar{V}$ values significantly different from the literature values, a gravimetric determination of the E^{280}_{1cm} was deemed necessary. Three solutions of BSA in distilled water (prepared as in Section IV D) were used in this determination. The absorbance of each solution was measured using a Gilford Model, 220 light detecting system, at a wave length of 280 nm as indicated on the Beckmann Model DUR light source. Samples of each solution were weighed out in triplicate and corrected to volumes using the density of each solution. The nine samples were dried in vaccuo at approximately 100°C. Completeness of drying was checked by weighing samples once and weighing them again after eight more hours in the oven under vacuum. The results are shown in Table XV and plotted in Figure 26. These values gave an extinction coefficient of $E^{280}_{1cm} = (6.136 \pm .057)$ $(percent)^{-1}$. This error could account for the differences in $\bar{V}_{[BSA]}$ in water values.

TABLE XV

Determination of the Bovine Serum Albumin Extinction Coefficient

Concentration of BSA (gm/ml)	Relative Error	A_{280}
0.003971	±2.1%	2.437
0.001286	±0.93%	0.791
0.000365	±26.0%	0.242
0.0000	±0.00%	0.000

FIGURE 26: A plot of Table XV showing BSA concentration as a function of absorbance at a wavelength of 280 nm.

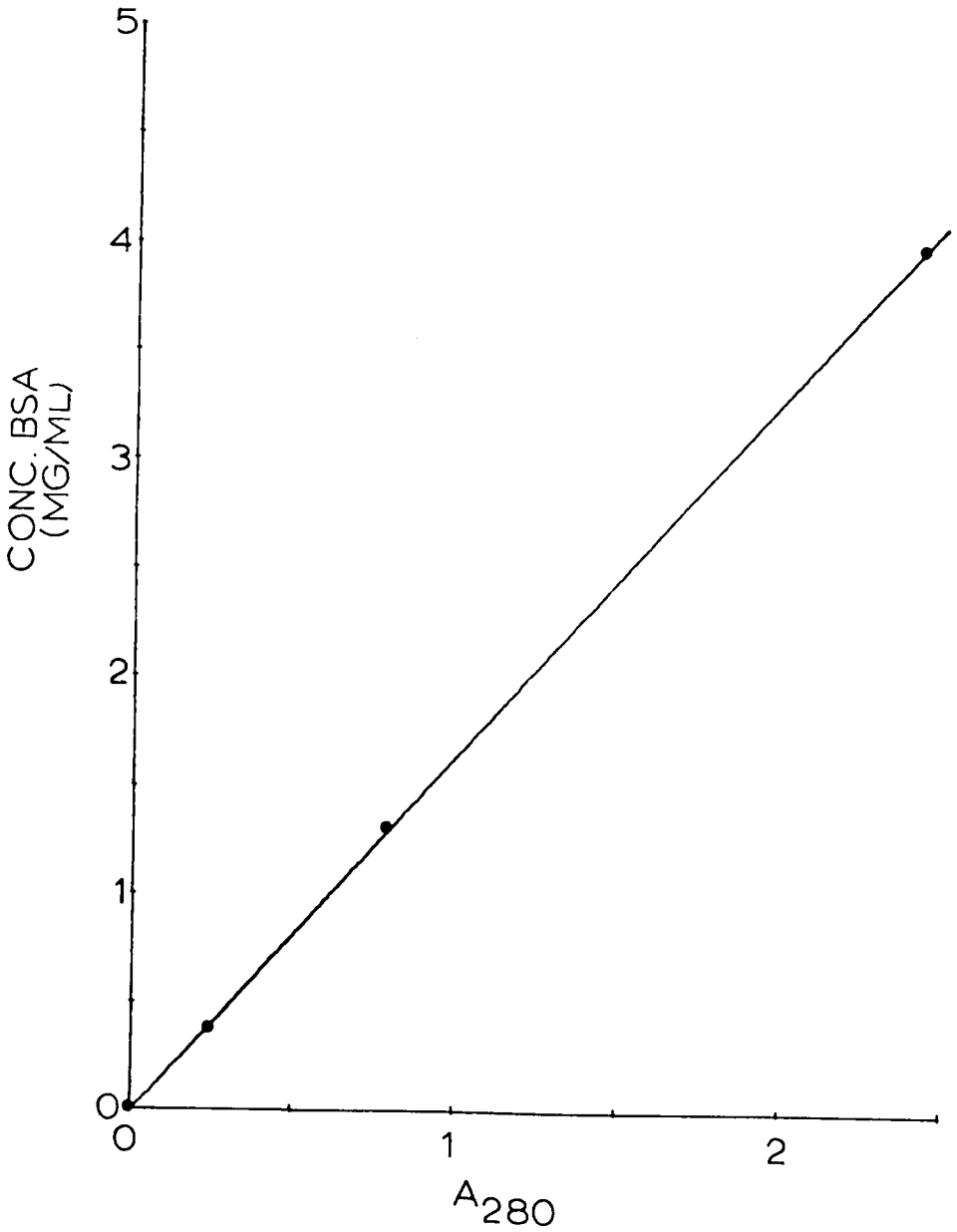
5
4
3
2
1
0
0
1
2
CONC. BSA
(MG/ML)
A280

REFERENCES

1. J. W. Beams, R. D. Boyle and P. E. Hexner, "Magnetically Suspended Equilibrium Ultra Centrifuge," Rev. Sci. Instr. 32, 645 (1961).

2. J. P. Senter, "Magnetic Densimeter Using Optical Sensing," Rev. Sci. Instr. 40, 334 (1969).

3. D. W. Kupke, "Volume Changes by Magnetic Densitometry," in Federation Proceedings, Symposia and Reports (Federation of American Societies for Experimental Biology, Washington, D. C., 1966) Vol. 25, p. 990.

4. D. W. Kupke, "Density and Volume Change Measurements," in Physical Principles and Techniques of Protein Chemistry, Part C (S. J. Leach, ed.) (New York: Academic Press, Inc., in press).

5. J. W. Beams and A. M. Clarke, "Magnetic Suspension Balance Method for Determining Densities and Partial Specific Volumes," Rev. Sci. Instr. 33, 750 (1962).

6. D. L. Deardorff and D. V. Ulrich, Bridgewater College, Bridgewater, Virginia, Personal Communication.

7. D. V. Ulrich, Dissertation, University of Virginia, Charlottesville, Virginia.

8. S. P. Almeida and T. H. Crouch, "Magnetic Densimeter Using an r f Sensing Coil," Rev. Sci. Instr. 42, 1344 (1971).

9. Circular of the National Bureau of Standards, No. 19, Oct. 31, 1924.

10. G. Cohen and H. Eisenberg, "Deoxyribonucleate Solutions: Sedimentation in a Density Gradient, Partial Specific Volumes, Density and Refractive Index Increments, and Preferential Interactions," Biopolymers 6, 1077 (1968)

11. T. H. Crouch, "The Effect of DCA on Poly-γ-Benzyl-L-Glutamate in DCE," (unpubl.)

12. F. E. Karasz and J. M. O'Reilly, "Volume Changes Accompanying the Helix-Coil Transition in Poly-γ-Benzyl-L-Glutamate," J. Phys. Chem. 71, 1159 (1967).

13. J. Steinhardt and J. A. Reynolds, Multiple Equilibria in Proteins (New York: Academic Press, Inc., 1969) p. 28.

14. H. A. Sober, Handbook of Biochemistry and Molecular Biology (Cleveland: Chemical Rubber Co., 1970) p. C-28.

15. E. E. Brumbach and G. K. Akers, "Molecular Sieve Studies of Interacting Protein Systems VII: Direct Optical Scanning Method for Ligand-Macromolecule Binding Studies," Anal. Biochem. 41, 543 (1971).

The vita has been removed from the scanned document

MAGNETIC DENSIMETERS: DESIGN AND OPERATION

Thomas Hafford Crouch

ABSTRACT

Presented here is a comparison of two magnetic densimeters, one using a r.f. sensing system and one using an optical sensing system. Both systems have the same control system. Based on a series of experiments, it appears that the optical sensing densimeter is much easier to handle than the one using r.f. sensing. This is because the r.f. system is much more sensitive to stray electromagnetic radiation.

Presented here also is a method for determining the partial specific volumes of each component in a multicomponent system, prior to and after the interaction of these components using a magnetic densimeter.